PREDICTED IMPACTS FROM OFFSHORE PRODUCED WATER DISCHARGES ON HYPOXIA IN THE GULF OF MEXICO

Final Report

EPA Contract No. 68-C-03-041
Work Assignment No. 3-01, Task 10

July 21, 2006

Prepared for:

U.S. Environmental Protection Agency
Region 6 (6WQ-PP)
1445 Ross Avenue
Dallas, TX 75202

Through:

Oceans and Coastal Protection Division
U.S. Environmental Protection Agency
1200 Pennsylvania Ave., NW
Washington, D.C. 20460

Prepared by:

Limno-Tech, Inc.
2109 Rolling Road
Greensboro, NC 27403
(336) 274-2688
E-mail: vbierman@limno.com

Through:

BATTELLE
397 Washington Street
Duxbury, MA 02332
(781) 934-0571

TABLE OF CONTENTS

List of Figures

List of Tables

EXECUTIVE SUMMARY

Summer hypoxia in the bottom waters of the northern Gulf of Mexico has received considerable scientific and policy attention because of potential ecological and economic impacts from this very large zone of low oxygen, and because of the implications for management within its massive watershed (Turner and Rabalais 1994, CENR 2000, Task Force 2001, Mitsch et al. 2001, Rabalais et al. 2002). An assessment of hypoxia causes and consequences (CENR 2000, Rabalais et al. 2002) concluded that the almost 3-fold increase in nitrogen load to the Gulf (Goolsby et al. 2001) is the primary external driver that stimulated the increase in hypoxia since the middle of the last century.

The Federal-State-Tribal Action Plan for reducing, mitigating, and controlling hypoxia in the northern Gulf of Mexico (Task Force 2001) included a goal of reducing the five-year running average size of the hypoxic zone to below 5,000 km^2 by 2015. After the Action Plan was developed, a new question arose as to whether sources other than the Mississippi River Basin (MRB) may also contribute significant quantities of oxygen-demanding substances. One very visible potential source is the hundreds of offshore oil and gas platforms located within or near the hypoxic zone. Many of these platforms discharge varying volumes of produced water. Produced water is trapped in underground formations and is brought to the surface along with oil or gas.

In response to a request by EPA in 2004, industry conducted a waste characterization study of produced water discharges to the Gulf of Mexico hypoxic zone (Veil et al. 2005). Produced water loadings of total nitrogen and total phosphorus for the entire hypoxic zone were estimated to be 15,061 and 109 lb/day, respectively, and are several orders of magnitude lower than those from the MRB. Produced water loadings of ammonia nitrogen were estimated to be 7.4 percent of those from the MRB; however, ammonia nitrogen loadings from the MRB are only 2 percent of the total nitrogen loadings from the MRB.

The objectives of this study were to assess the incremental impacts of produced water discharges on dissolved oxygen conditions in the northern Gulf of Mexico, and to evaluate the significance of these discharges relative to loadings from the MRB. This study was conducted using three existing models of Gulf hypoxia developed by Bierman et al. (1994), Justić et al (1996, 2002) and Scavia et al. (2003). Results from this study will provide EPA with an initial assessment of the appropriate forward path for how to incorporate produced water discharges within the overall framework for controlling nutrient loadings to the Gulf of Mexico as a management tool for reducing the occurrence and extent of hypoxia.

The study approach involved conducting predictive simulations with the original Bierman, Justić and Scavia models using the estimated produced water loads developed by Veil et al. (2005). All model coefficients, including those representing degradation, decay, recycle and settling were kept the same as in the original models. The produced water loads were organized for each model to be compatible with their conceptual frameworks, state variables, and spatial scales. All produced water loads were assumed to be constant in time. Scenarios were designed for each model that addressed loading uncertainties, settleability of suspended BOD and TOC, and, for

the Justić and Scavia models, different assumptions on delivery locations for the produced water loads.

Results from the Bierman model for predicted average percent changes in bottom water dissolved oxygen concentrations for 1985, 1988 and 1990 ranged from -0.110 to -0.201 percent for base produced water loads. The largest range across all of the lower- and upper-bound predictive simulations was from -0.091 to -0.237 percent.

In the original predictions from the Justić model, bottom waters went hypoxic in 19 of 45 years from 1955 to 2000. In this study, there were no changes in frequency of hypoxia for any of the predictive simulations with produced water loads. Bottom waters still went hypoxic in 19 of 45 years for all simulations. Furthermore, there were no changes in the number of months in which the bottom waters went hypoxic between the original predictions and the predictive simulations in this study.

Results from the Justić model for predicted average percent changes in bottom water dissolved oxygen concentrations were -0.0023 percent for base produced water loads delivered at the Mississippi delta, and ranged from -0.067 to -0.513 percent for these loads delivered at a 10 x 10 km grid located in the core of the hypoxic zone. The largest range across all of the lower- and upper-bound predictive simulations was from -0.0017 to -0.660 percent.

The Scavia model predicted that for base produced water loads delivered at the Mississippi and Atchafalaya Rivers, hypoxic area would increase by an average of 4.5 percent in 3 of 18 years from 1985-2002. The predicted increase in actual hypoxic area for all three years was 331 km^2. For these same loads delivered at 20 km intervals along the spine of the hypoxic zone, the Scavia model predicted that hypoxic area would increase by an average of 3.1 percent in 2 of the 18 years. The predicted increase in actual hypoxic area for these two years was 331 km^2.

All of the predictive results in this study contain uncertainties inherent in each of the original models, in addition to the uncertainties explicitly considered for the produced water loads. Despite uncertainties in model results for absolute magnitudes of dissolved oxygen concentrations and hypoxic areas, relative differences between baseline and predictive simulations have higher degrees of confidence because the absolute uncertainties tend to be self-cancelling. The predicted incremental impacts of produced water loads on dissolved oxygen conditions in the northern Gulf of Mexico from all three models were small. Even considering the predicted ranges between lower- and upper-bound results, these impacts are likely to be within the errors of measurement for bottom water dissolved oxygen and hypoxic area at the spatial scale of the entire hypoxic zone.

INTRODUCTION

Summer hypoxia in the bottom waters of the northern Gulf of Mexico has received considerable scientific and policy attention because of potential ecological and economic impacts from this very large zone of low oxygen, and because of the implications for management within its massive watershed (Turner and Rabalais 1994, CENR 2000, Task Force 2001, Mitsch et al. 2001, Rabalais et al. 2002). These regions of oxygen concentrations below 2 mg/L that form off the Louisiana coast each spring and summer increased from an average of 8,300 km^2 in 1985–

1992 to over 16,000 km^2 in 1993–2001 (Rabalais et al. 2002), and reached a record 22,000 km^2 in 2002. There is significant inter-annual variability and no comprehensive records of areal extent exist prior to 1985. Figure 1 is a composite plot that shows the frequency of occurrence of mid-summer hypoxia in the Gulf of Mexico from 1985 to 1999.

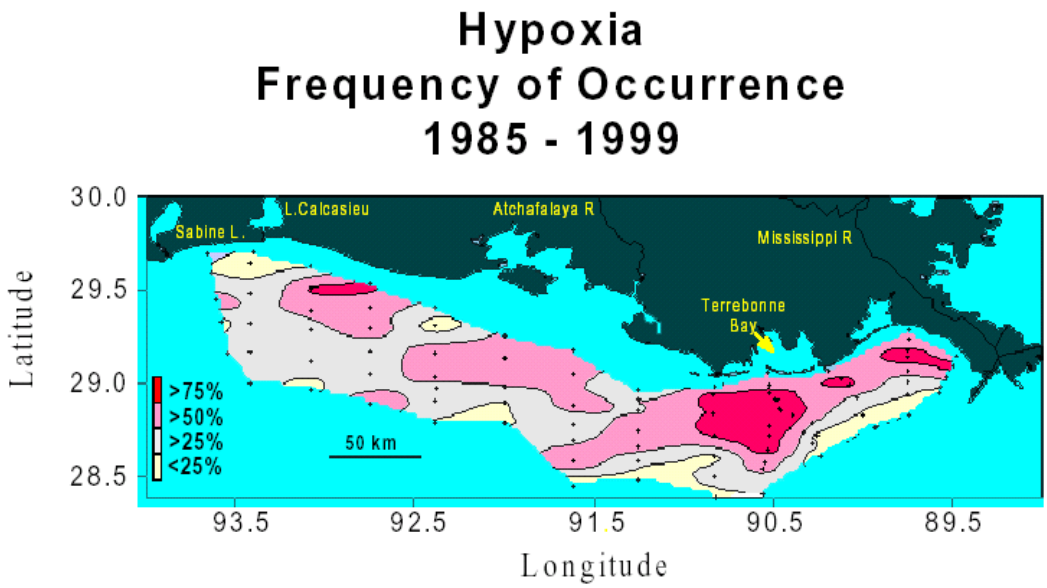

Figure 1. Frequency of occurrence of mid-summer hypoxia in the Gulf of Mexico – based on data from Rabalais, Turner and Wiseman (CENR 2000).

An assessment of hypoxia causes and consequences (CENR 2000, Rabalais et al. 2002) concluded that the almost 3-fold increase in nitrogen load to the Gulf (Goolsby et al. 2001) is the primary external driver that stimulated the increase in hypoxia since the middle of the last century. This riverine nitrogen input stimulates coastal algal production and the subsequent settling of organic matter below the pycnocline. Because the pycnocline inhibits vertical oxygen flux, decomposition of organic matter below the pycnocline consumes oxygen faster than it is replenished, resulting in declining oxygen concentrations during the period of stratification.

The Federal-State-Tribal Action Plan for reducing, mitigating, and controlling hypoxia in the northern Gulf of Mexico (Task Force 2001) included a goal of reducing the five-year running average size of the hypoxic zone to below 5,000 km^2 by 2015. After the Action Plan was developed, a new question arose as to whether sources other than the Mississippi River Basin (MRB) may also contribute significant quantities of oxygen-demanding substances. One very visible potential source is the hundreds of offshore oil and gas platforms located within or near the hypoxic zone. Many of these platforms discharge varying volumes of produced water. Produced water is trapped in underground formations and is brought to the surface along with oil or gas.

Figure 2 (J.P. Smith, ExxonMobil Upstream Research Company, personal communication) shows the frequency of occurrence of mid-summer hypoxia superimposed on a lease block map of the Gulf of Mexico. The blue dots on the map show platforms in the region. There are an estimated 287 platforms in the hypoxia zone (Veil et al. 2005); however, not every platform is a produced water discharge point. The red boxes indicate the lease block areas that are in the hypoxic zone. Each box is marked with the number of lease blocks in the area that have produced water discharges and that are in the hypoxic zone.

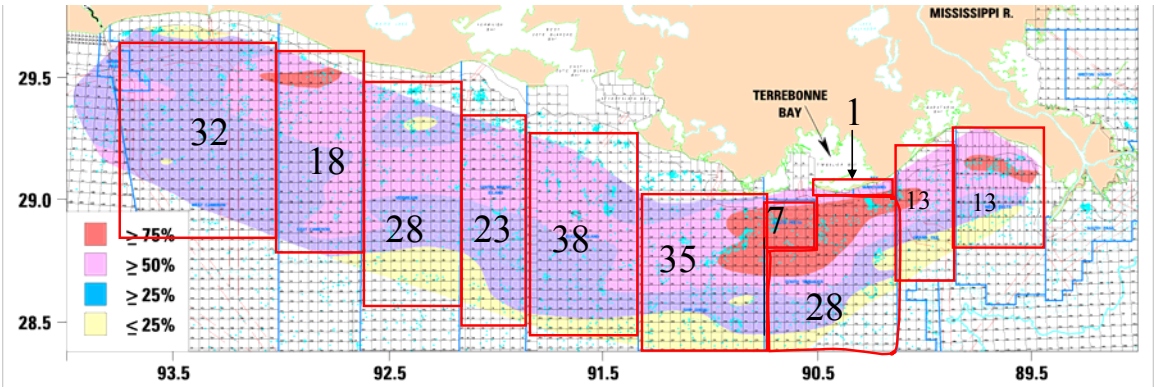

Figure 2. Map of hypoxic zone showing numbers and locations of oil and gas platforms.

Until recently, only limited data characterizing oxygen demand, nutrient concentrations and loadings from offshore produced water discharges had been collected. These discharges are part of the EPA National Pollutant Discharge Elimination System (NPDES) and are included in a general permit. As part of the re-issuance of this permit in 2004, EPA requested that the industry provide information on the amount of oxygen-demanding substances contained in the produced water discharges.

OBJECTIVES

The objectives of this study were to assess the incremental impacts of produced water discharges on dissolved oxygen conditions in the northern Gulf of Mexico, and to evaluate the significance of these discharges relative to loadings from the MRB. This study was conducted using the three existing models of Gulf hypoxia described in Scavia et al. (2004). Results from this study will provide EPA with an initial assessment of the appropriate forward path for how to incorporate produced water discharges within the overall framework for controlling nutrient loadings to the Gulf of Mexico as a management tool for reducing the occurrence and extent of hypoxia.

EXISTING MODELS OF GULF HYPOXIA

The three existing models of Gulf hypoxia (Bierman et al. 1994; Justić et al. 1996, 2002; Scavia et al. 2003) capture very different aspects of the physics, chemistry, biology and ecology of the northern Gulf. Table 1 contains a summary of the principal attributes of each model in terms of spatial and temporal scales, nutrients, characterization of hypoxia and calibration time periods.

Table 1. Principal Attributes of Gulf of Mexico Hypoxia Models

Attribute	MODEL		
	Bierman	**Justić**	**Scavia**
General Description	Moderately complex mechanistic eutrophication model	Simple two-layer dissolved oxygen model	Simple dissolved oxygen model for bottom waters
Spatial Scale	3D with 21 spatial segments in hypoxic zone	1D vertical at Station C6 in core of hypoxic zone	1D horizontal in subpycnocline downstream of river inputs
Temporal Scale	Summer Steady-State	Monthly Time-Variable	Summer Steady-State
Nutrients	Phosphorus, nitrogen and silicon	Nitrogen	Nitrogen
Hypoxia Characterization	3D structure of summer-average dissolved oxygen concentrations in hypoxic zone	Seasonal dynamics of dissolved oxygen concentrations in core of hypoxic zone	Interannual variability in hypoxic zone length and area
Calibration Time Periods	1985, 1988 and 1990	1985-1993	1985-2002

Table 2 contains a summary of the state variables in each model. Mass balances are conducted for each of these state variables, which correspond to the individual water quality parameters. The basic outputs for each model are spatial and/or temporal concentration distributions for each of these water quality parameters.

Table 2. Model State Variables for Gulf of Mexico Hypoxia Models

State Variables	MODEL		
	Bierman	Justić	Scavia
Dissolved Oxygen	X	X	X
Biochemical Oxygen Demand (BOD)	X		X
Sediment Organic Carbon		X	
Salinity	X		
Algal Carbon	X		
Phosphate Phosphorus	X		
Organic Phosphorus	X		
Ammonium Nitrogen	X		
Nitrate/Nitrite Nitrogen	X		
Organic Nitrogen	X		

Bierman Model

The most complex model (Bierman et al. 1994) simulates summer steady-state, three-dimensional, food-web-nutrient-oxygen dynamics (Figure 3). This model is based on a version of the U.S. EPA Water Analysis Simulation Program (WASP) adapted to a 21-segment, three-dimensional spatial grid on the Louisiana-Texas shelf. State variables include salinity, phytoplankton, phosphorus, nitrogen, dissolved oxygen, and carbonaceous biochemical oxygen demand. The model is driven by externally-specified values for nutrient loadings, water circulation, seaward and sediment boundary conditions, temperature, incident solar radiation, and underwater light attenuation. Water circulation was derived from a salinity mass balance.

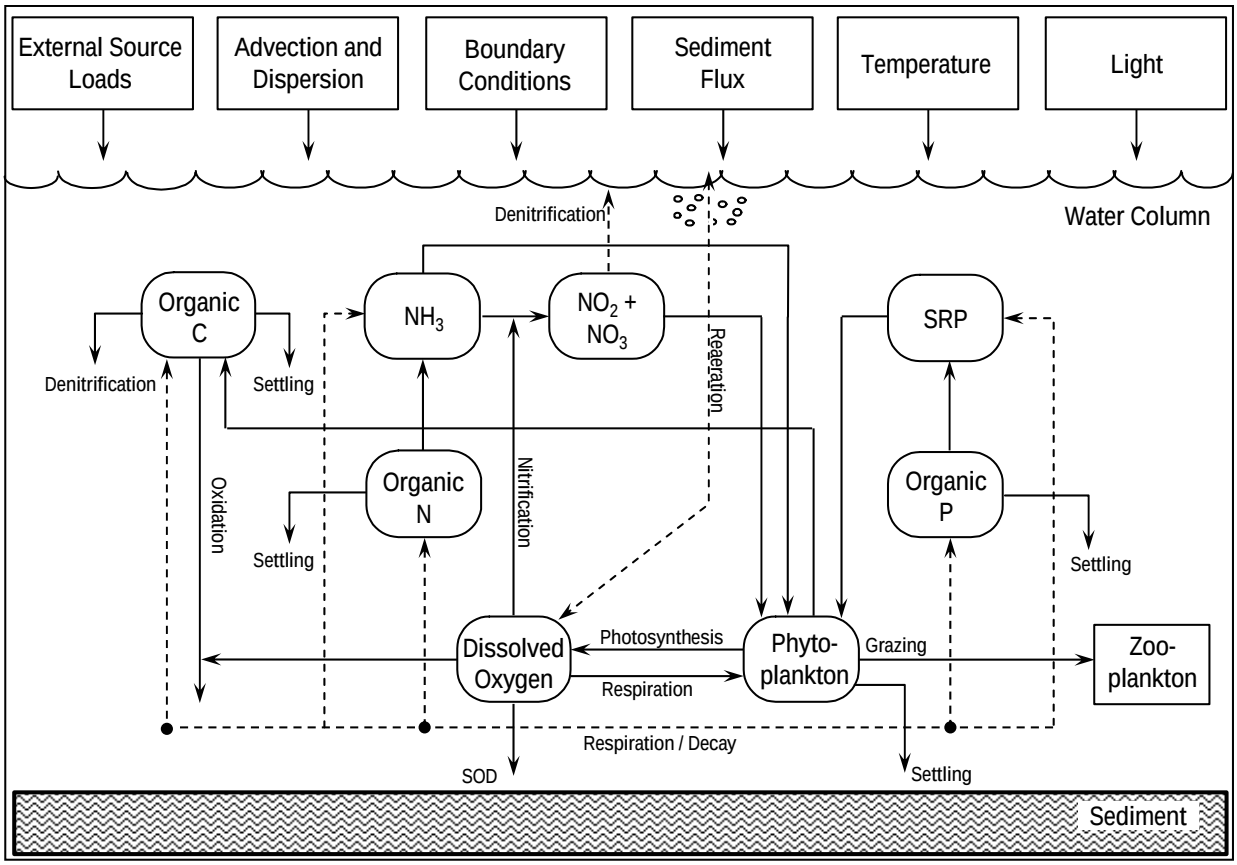

Figure 3. Bierman et al. (1994) model conceptual framework.

The model was initially calibrated to a comprehensive set of field data collected during July 1990 at over 200 stations in the northern Gulf of Mexico. Reasonable values were obtained between computed and observed values for model state variables, primary production and particulate carbon and nitrogen settling rates. Figure 4 is an example of model calibration results for nitrate nitrogen concentrations in surface waters and dissolved oxygen concentrations in subpycnocline waters.

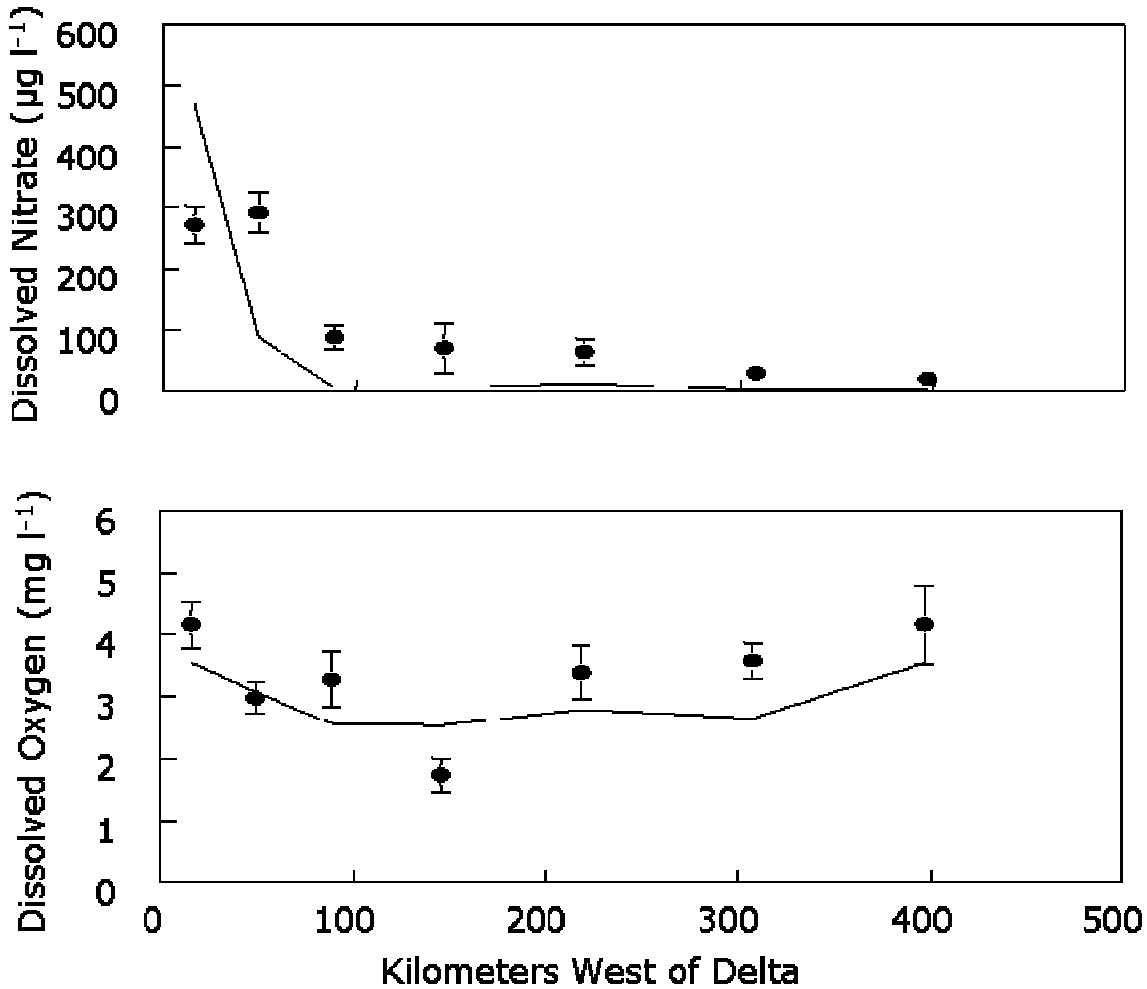

Figure 4. Bierman model calibration results for mid-summer surface nitrate and bottom water dissolved oxygen concentrations.

Subsequently, the model calibration was extended to include data collected during 1985 and 1988. Results indicated no significant differences between overall mean values for model output and field data for almost all state variable-year combinations for 1985, 1988, and 1990. The calibrated model was used to forecast potential responses of dissolved oxygen concentrations to reductions in nutrient loads from the MRB (Limno-Tech, Inc. 1995). To address uncertainties due to differences in hydrometeorological conditions, forecasts were conducted for 1985, 1988 and 1990 calibration conditions for each nutrient load reduction.

Justić Model

A simpler model (Justić et al. 1996, 2002) simulates two-layer, time-dependent, oxygen dynamics (Figure 5) for one location off the Louisiana coast, driven by meteorological conditions and nitrogen loads. The model is represented by a system of three coupled, non-

linear, ordinary differential equations. The first equation describes changes in the average oxygen concentration of the upper water column (0-10 m), the second differential equation describes changes in the sedimentary pool of organic carbon, and the third differential equation describes changes in the average oxygen concentration of the lower water column (10-20 m). Model forcing functions include monthly values of the Mississippi River runoff, nitrate concentration, nitrate flux, ambient water column temperature, and surface winds. A detailed description of the model governing equations, state variables, model parameters and forcing functions is given in Justić et al. (1996, 2002).

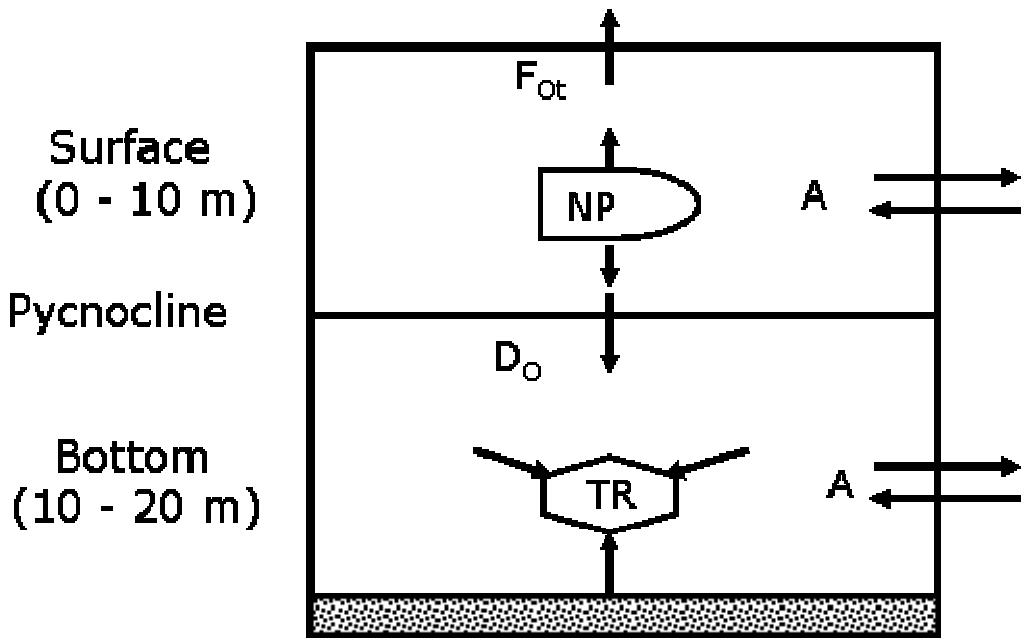

Figure 5. A conceptual model of oxygen cycling in the core of the Gulf's hypoxic zone (from Justić et al., 1996, reprinted with permission of American Society of Limnology and Oceanography). The F_{Ot} denotes the total air-sea oxygen flux, *NP* is the net productivity of the upper layer, D_O is the diffusive oxygen flux through the pycnocline, *A* is the horizontal oxygen transport by advection and diffusion, and *TR* is the total oxygen uptake in the lower water column.

The model was calibrated using the 1985-1993 time-series for a station within the core of the hypoxic zone (Figure 6). This period included three average hydrologic years (1985, 1986, and 1989), a record flood year (1993), two years with above average discharge (1990 and 1991), three years with below average discharge (1987, 1988, and 1992), and a record drought year (1988). Given this time span and range of hydrologic variability, this data set was deemed appropriate for model calibration. A sensitivity analysis revealed that the model is highly sensitive to external forcing, yet sufficiently robust to remain stable and reproduce observed dynamics under an order of magnitude change in the nitrate flux between successive months,

such as those encountered during the flood of 1993 (Justić et al. 2002). After calibration, the model was used to simulate and hindcast seasonal oxygen concentrations from 1955 to 2000, linking decadal changes in the MRB nutrient load to eutrophication near the Mississippi River delta. It was also extended and used (Justić et al. 2003) to simulate potential impacts of climate change on the development of annual hypoxia.

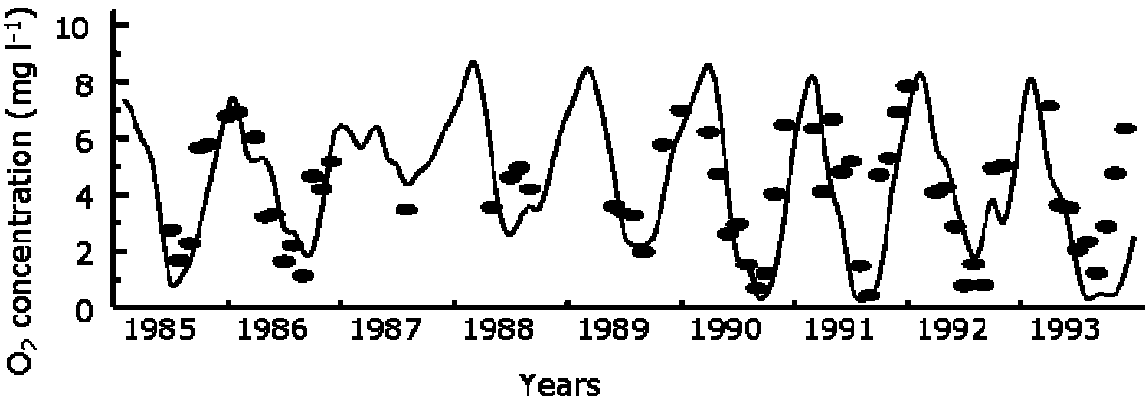

Figure 6. Observed (dots) and predicted (solid line) monthly averages (June 1985-November 1993) of bottom (10-20 m) oxygen concentrations at station C6A within the core of the Gulf of Mexico hypoxic zone.

Scavia Model

The simplest model (Scavia et al. 2003) simulates summer steady-state, one-dimensional horizontal dynamics of nutrient-dependent production, respiration of organic matter, and resulting oxygen balance (Figure 7). It is driven by May-June total nitrogen loads, calibrated to 17 years of data between 1985 and 2002, and used to simulate, hindcast, and forecast hypoxic zone length and area in response to changes in nitrogen loads. This model was the first to successfully predict effects of variable nutrient loads directly on the areal extent of hypoxia on the Louisiana-Texas shelf. An adaptation of a model used extensively for rivers and estuaries (e.g., Chapra 1997), the model simulates concentrations of subpycnocline oxygen-consuming organic matter and dissolved oxygen downstream from the Mississippi and Atchafalaya rivers. Scavia et al. (2003) discussed the validity of assumptions of steady-state and no dispersion, as well as those of surface and bottom water movement being constrained such that the subpycnocline water movement can be modeled as one-dimensional flow, May-June river total nitrogen load can be used as a surrogate for the organic matter load below the pycnocline, and subpycnocline oxygen consumption and cross-pycnocline oxygen flux can be modeled as first-order processes.

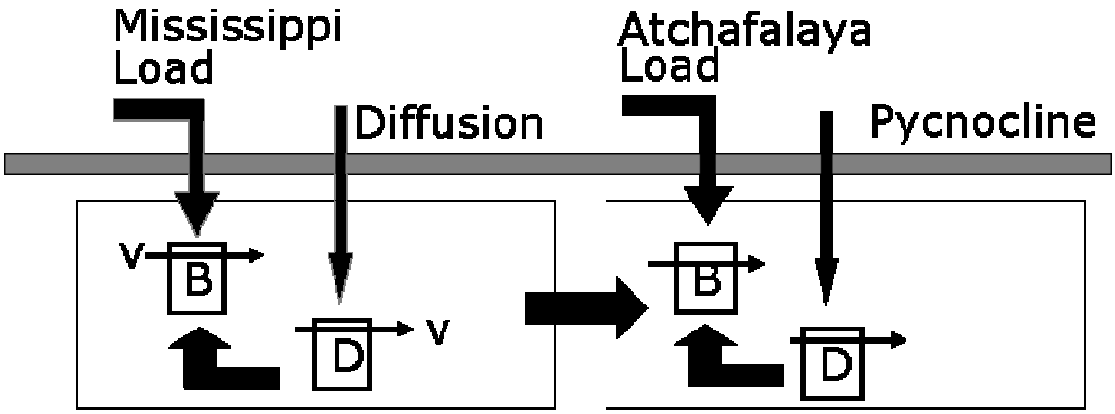

Figure 7. Scavia model conceptual framework (from Scavia et al. 2004, reprinted with permission of Estuarine Research Federation). B represents biochemical oxygen demand, D represents dissolved oxygen, and v is net downstream advection.

The calibrated model explains 95 percent of 1985-2002 interannual variation in hypoxic zone length and 88 percent of hypoxic zone area (Figure 8). Because they could not fully parameterize historical oceanographic effects and because it is impossible to determine future values for that effect, Scavia et al. (2003) developed probabilistic hindcasts and forecasts based on assumed probability distributions for subpycnocline, net long-shore advection, and Monte Carlo analysis.

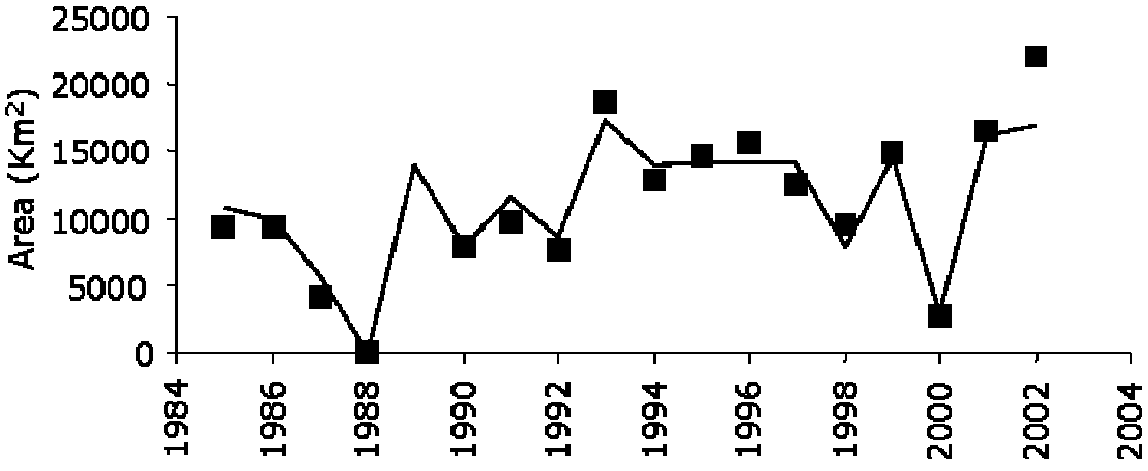

Figure 8. Observed (solid boxes) and predicted (solid line) of hypoxia area (from Scavia et al. 2003).

LOADINGS FROM PRODUCED WATERS

In response to a request by EPA in 2004, industry conducted a waste characterization study of produced water discharges to the Gulf of Mexico hypoxic zone (Veil et al. 2005). This study involved a program to sample 50 offshore oil and gas platforms located within the hypoxic zone. The loadings for the 50 sampled platforms represent a produced water discharge volume of approximately 176,000 bbl/day. The total amount of produced water generated in the hypoxic zone during 2003 was estimated as 508,000 bbl/day. This volume was based on annual reports by operators to the Minerals Management Service. It reflects the volume of produced water that is generated from each lease, not the volume that is discharged from each platform.

The mass loadings from offshore oil and gas discharges to the entire hypoxic zone were estimated by multiplying the 50-platform loadings by the ratio of total water generated to the 50-platform discharge volume. The produced water loadings for the entire hypoxic zone are summarized in Table 3. To provide regional context, Table 3 also includes estimated mass loadings delivered to the Gulf from the MRB during 1980-1996. The produced water loadings of total nitrogen and total phosphorus for the entire hypoxic zone are 15,061 and 109 lb/day, respectively, and are several orders of magnitude lower than those from the MRB. Produced water loadings of ammonia nitrogen are 7.4 percent of those from the MRB; however, ammonia nitrogen loadings from the MRB are only 2 percent of the total nitrogen loadings from the MRB.

Table 3. Relative Contributions of Loadings from Produced Waters

Parameter	Mean Daily Loads from MRB to Gulf of Mexico, 1980-1996* (lbs/day)	Estimated Mean Daily Loads from Produced Waters to Gulf of Mexico Hypoxic Zone** (lbs/day)	Percent Contributions of Produced Waters
Total N	9,470,000	15,061	0.16
Nitrate N	5,750,000	197	0.003
Ammonia N	187,000	13,804	7.38
Total P	824,000	109	0.013
Orthophosphate P	252,000	65	0.026

*adapted from Goolsby et al. 1999
**adapted from Veil et al. 2005

DEVELOPMENT OF MODEL SCENARIOS

Approach

The study approach involved conducting predictive simulations with the original Bierman, Justić and Scavia models using the estimated produced water loads developed by Veil et al. (2005). All model coefficients, including those representing degradation, decay, recycle and settling were kept the same as in the original models. The produced water loads were organized for each model to be compatible with their conceptual frameworks, state variables, and spatial scales. All produced water loads were assumed to be constant in time. Scenarios were designed for each model that addressed loading uncertainties, settleability of suspended BOD and TOC, and, for the Justić and Scavia models, different assumptions on delivery locations for the produced water loads.

Results for the Bierman and Justić models are presented in terms of bottom water dissolved oxygen concentrations. Results for the Scavia model are presented in terms of area of hypoxia. Results for each model correspond to the incremental impacts of produced water loads, relative to results from the original models which included only loads from the MRB. These incremental impacts are reported in terms of percent change and absolute change.

Spatial Scales

The spatial scale of the assessment study is shown in Figure 9. The indicated hypoxic zone corresponds to the spatial area for which there is greater than a 25 percent frequency of occurrence of hypoxia (Figure 1). This is the operational definition of the hypoxic zone for the estimated produced water loads in Veil et al. (2005). The indicated oil and gas lease blocks correspond to the lease blocks in Figure 2 that lie within this hypoxic zone.

The spatial domain of the Bierman model is represented by a 21-segment grid extending from the Mississippi River delta west to the Louisiana-Texas border, and from the shoreline seaward to the 30-60 m bathymetric contours. The 14 model grid cells shown in Figure 9 correspond to the surface water segments in the model. The spatial grid includes one vertical layer nearshore and two vertical layers offshore. The nearshore segments have an average depth of 5.6 m. The surface offshore segments are completely mixed in the vertical to a fixed pycnocline depth of 10 meters. The bottom offshore segments are completely mixed from 10 meters to the seabed. The depths of these bottom offshore segments range between 6.1 and 20.3 meters. All predictive simulations with the Bierman model involved apportionment of the total produced water loads into individual model segments, depending on lease block locations and discharge depths.

Unlike the Bierman model, the spatial domains of the Justić and Scavia models did not completely coincide with all of the lease block locations in the hypoxic zone. Assumptions were required for each of these models on delivery points for the produced water loads. The scale at the bottom of Figure 9 indicates 20 km intervals along the spine of the hypoxic zone. For one set of predictive simulations with the Scavia model, total produced water loads were split into separate delivery points at the Mississippi and Atchafalaya Rivers, the delivery points in the original application of the model. Produced water loads from lease blocks between the Mississippi and Atchafalaya Rivers were delivered at the Mississippi delta, and produced water loads from lease blocks west of the Atchafalaya River were delivered at the Atchafalaya River

mouth. For another set of predictive simulations with the Scavia model, total produced water loads were apportioned to 23 delivery points at the indicated 20 km intervals, depending on lease block locations. This scenario is a more realistic representation of the actual delivery points for produced water loads within the framework of the Scavia model.

Figure 10 shows spatial detail in the vicinity of Station C6, the monitoring station used for calibration of the Justić model. For one set of predictive simulations with the Justić model, produced water loads from lease blocks between the Mississippi delta and Station C6 were assumed to be delivered at the Mississippi River, the delivery point in the original application of the model. For another set of predictive simulations, produced water loads from lease blocks located within a 10 x 10 km grid centered on Station C6 were assumed to be delivered at Station C6. This scenario represents potential impacts at Station C6 due to near-field produced water loads. In contrast to the Bierman and Scavia models, which were both run with the total produced water loads, these two scenarios with the Justić model were run with only 47 and 8 percent, respectively, of the total produced water loads.

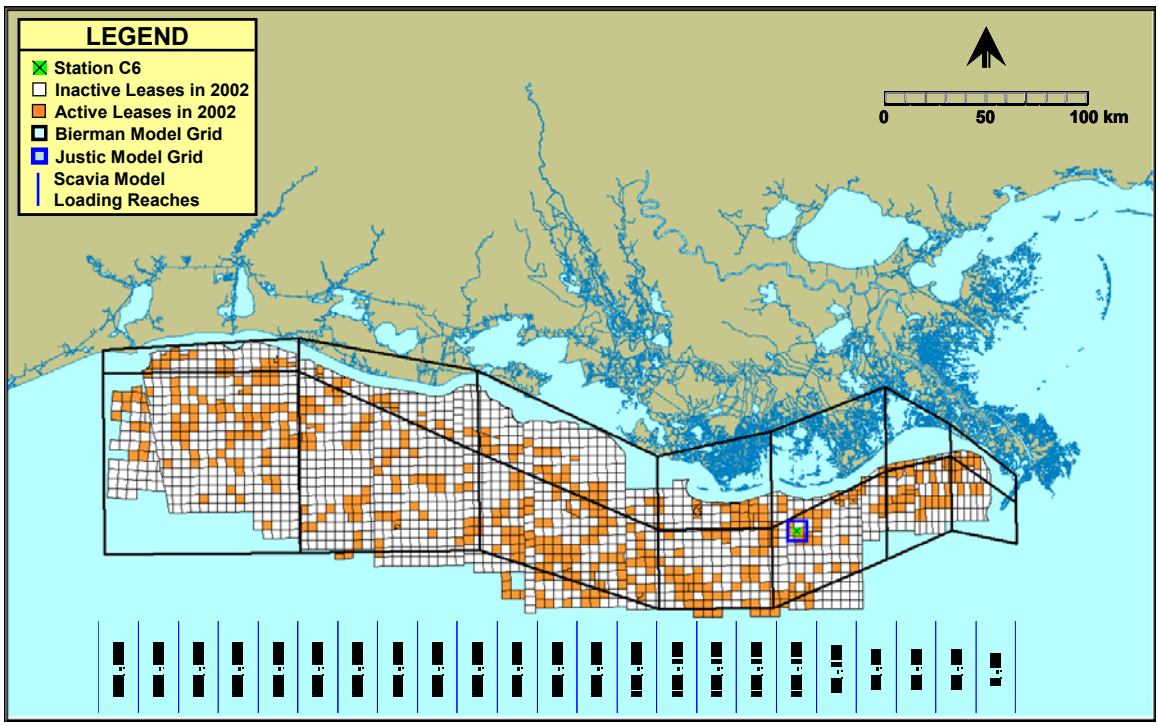

Figure 9. Hypoxic zone on the Louisiana-Texas Shelf showing oil and gas lease blocks, locations of Bierman model grid cells, Station C6 for the Justić model, and loading intervals along the spine of the hypoxic zone for the Scavia model.

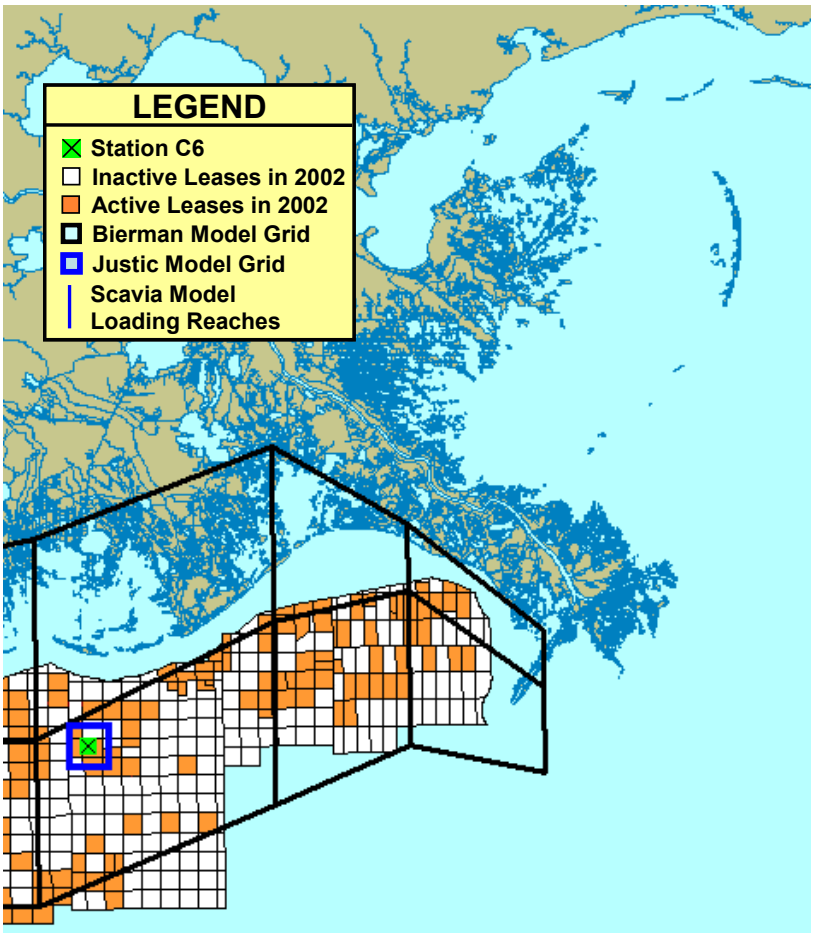

Figure 10. Spatial detail in the vicinity of Station C6 for the Justić model.

Assumptions

In addition to the above assumptions on delivery points for produced water loads, the following additional assumptions were made for each of the three models:

- All of the produced water generated from each lease block is actually discharged.
- All produced water loads were assumed to be constant in time.
- Ultimate BOD (BOD_U) is equal to 1.25 times reported five-day BOD (BOD_5).
- The "suspended phase" fractions of BOD and TOC are 15 percent.
- Sixty-eight (68) percent of total produced water volume for the hypoxic zone is discharged to surface waters (0-10 meters) and 32 percent is discharged to bottom waters (below 10 meters).

The assumption that all produced water generated is actually discharged is consistent with Veil et al. (2005). Produced water loads in Veil et al. (2005) correspond only to current conditions. These loads were developed using chemical concentrations measured in 2005 and produced water volume generated in 2003. There are insufficient data to develop produced water loads for earlier historical conditions. Consequently, produced water loads were assumed to be constant in time for all of the predictive simulations in this study.

The assumptions for BOD_U and the "suspended phase" fractions of BOD and TOC were based on information provided by the industry work group (Veil et al. 2006a). The assumed split between surface and bottom water discharges was developed using the OOC Hypoxia Registry database. The MMS Database on Produced Water Production by Lease during 2003 contains discharge volumes but no information on discharge depths. The OOC Hypoxia Registry database has information on discharge depths, but does not include all of the same discharges as the MMS database. Consequently, the assumed split between surface and bottom water discharges is an estimate using the best available data.

In the three original models it is assumed that the particulate phase fractions of BOD and TOC are settleable. If significant portions of the reported "suspended phase" BOD or TOC from produced waters are dispersed or colloidal oil droplets, then the settling characteristics of these "suspended phases" would be uncertain. To address this uncertainty, bounding simulations were conducted for these "suspended phase" produced water loads. As discussed above, the "suspended phase" was assumed to be 15 percent of the total reported produced water loads for both BOD and TOC. One bounding simulation assumed 100 percent settleability of this "suspended phase" and the other bounding simulation assumed zero settling of this phase.

Finally, to address uncertainties in produced water loads, bounding simulations were conducted at upper and lower 95 percent confidence intervals for each loading constituent. These confidence intervals were provided by the industry work group (Veil et al. 2006b). For each scenario and model, simulations were conducted with the following produced water loads:

- Base loads as reported in Veil et al. (2005).
- Lower bound loads = Base loads – 95% confidence interval for each constituent.
- Upper bound loads = Base loads + 95% confidence interval for each constituent.

Appendix A contains details of how the base loads were spatially organized and input to each of the three models.

Bierman Model Scenarios

A total of 18 predictive simulations were conducted with the Bierman model. For all simulations produced water (PW) loads were apportioned into individual model spatial segments, depending on lease block locations and discharge depths. Simulations were conducted for two settleability conditions:

- "Suspended phase" PW BOD settles.
- "Suspended phase" PW BOD does not settle.

Each of these settleability conditions included simulations with base, lower bound and upper bound PW loads and summer average, steady-state conditions for 1985, 1988 and 1990.

Justić Model Scenarios

A total of 9 predictive simulations were conducted with the Justić model. Simulations were conducted for two PW delivery locations:

- Mississippi Delta - PW loads (nitrate nitrogen) only from lease blocks between the Mississippi delta and Station C6. These loads represent 47 percent of the total PW loads to the hypoxic zone.
- 10 x 10 km grid centered on Station C6 - PW loads (nitrate nitrogen and TOC) only from lease blocks within this grid. These loads represent 8 percent of the total PW loads to the hypoxic zone.

Simulations were conducted for two settleability conditions:

- "Suspended phase" PW TOC settles (only for 10 x 10 km grid).
- "Suspended phase" PW TOC does not settle (only for 10 x 10 km grid).

Simulations for each delivery location and settleability condition were conducted with base, lower bound and upper bound PW loads and results are presented for monthly average bottom water dissolved oxygen concentrations from 1955-2000.

The original application of the Justić model assumed that all nitrate nitrogen loads were delivered at the Mississippi delta and the resulting net primary productivity in the surface waters created vertical carbon flux to the bottom waters. The original application did not include any representation of riverine TOC loads. Consequently, "suspended phase" TOC is not represented in the predictive simulations with the Justić model that assumed delivery of PW loads at the Mississippi delta.

The Justić model predictive simulations that assumed delivery of PW loads from lease blocks within the 10 x 10 km grid did include explicit representation of TOC. The rationale was that PW loads of TOC from within this grid would affect vertical carbon flux to the bottom waters,

and hence dissolved oxygen concentrations at Station C6. Consequently, the two settling conditions for "suspended phase" TOC were included in the Justić model predictions for PW loads delivered within the 10 x 10 km grid.

Scavia Model Scenarios

A total of 12 predictive simulations were conducted with the Scavia model. Simulations were conducted for two PW delivery locations:

- Total PW loads split into delivery points at the Mississippi and Atchafalaya Rivers.
- Total PW loads apportioned to 23 delivery points at 20 km intervals along the spine of the hypoxic zone.

Simulations were conducted for two settleability conditions:

- "Suspended phase" PW BOD settles from surface to bottom waters.
- "Suspended phase" PW BOD does not settle from surface to bottom waters.

Simulations for each delivery location and settleability condition were conducted with base, lower bound and upper bound PW loads and results are presented for summer average areal extent of hypoxia from 1985-2002.

The original application of the Scavia model assumed that total nitrogen load can be used as a surrogate for the organic matter load delivered to the bottom waters. Consistent with the approach used in the original application, PW loads of inorganic nitrogen to the surface waters were converted to settleable BOD in the form of algal cells, and then 50 percent of this algal BOD sinks below the pycnocline. In addition, it was assumed that PW loads of BOD (converted to BOD_U) delivered directly to the bottom waters also contributed to oxygen consumption.

SCENARIO RESULTS

Bierman Model

Table 4 contains predicted average percent changes in bottom water DO concentrations from the Bierman model for all scenarios. Each result corresponds to summer average, steady-state conditions, operationally defined as those occurring during July-August, the period during which annual hypoxia cruises are conducted by Dr. Nancy Rabalais and co-workers. Spatially, each result corresponds to the average percent change for the seven bottom water spatial segments in the model. As discussed below, these percent changes in bottom water DO concentrations are not constant in space, but vary over these seven spatial segments along the shelf contour. For base PW loads, results range from -0.110 to -0.201 percent for settling PW BOD and from -0.118 to -0.143 percent for non-settling PW BOD. The largest range across all of the lower- and upper-bound predictive simulations was from -0.091 to -0.237 percent.

Table 4. Predicted Average Percent Changes in Summer Bottom Water Dissolved Oxygen Concentrations from the Bierman Model.

	Produced Water (PW) Loads		
Scenario	**Base**	**Lower Bound**	**Upper Bound**
1985			
Suspended PW BOD Settles	-0.110	-0.091	-0.130
Suspended PW BOD Does Not Settle	-0.118	-0.099	-0.138
1988			
Suspended PW BOD Settles	-0.118	-0.097	-0.139
Suspended PW BOD Does Not Settle	-0.138	-0.117	-0.159
1990			
Suspended PW BOD Settles	-0.201	-0.165	-0.237
Suspended PW BOD Does Not Settle	-0.143	-0.107	-0.179

Figures 11-13 show predicted percent changes in bottom water DO concentrations from the Bierman model for 1985, 1988 and 1990, respectively, for individual model spatial segments along the shelf contour. Results are included for base, lower bound and upper bound PW loads, and for settling and non-settling PW BOD. For 1985 (Figure 11) and 1988 (Figure 12) the impacts of PW loads increase with distance from the delta and level off west of the Atchafalaya River, which is located 220 km downstream. There is little difference between results for settling and non-settling PW BOD near the delta, but impacts for non-settling PW BOD become greater west of the Atchafalaya. For 1990 (Figure 13) the results show different spatial patterns than for 1985 and 1988, and there are greater differences between results for settling and non-settling PW BOD. Predicted impacts for non-settling PW BOD increase with distance from the delta, but more sharply than those for 1985 and 1988. Predicted impacts for settling PW BOD are greater than those for non-settling PW BOD near the delta, but cross over and become smaller west of the Atchafalaya.

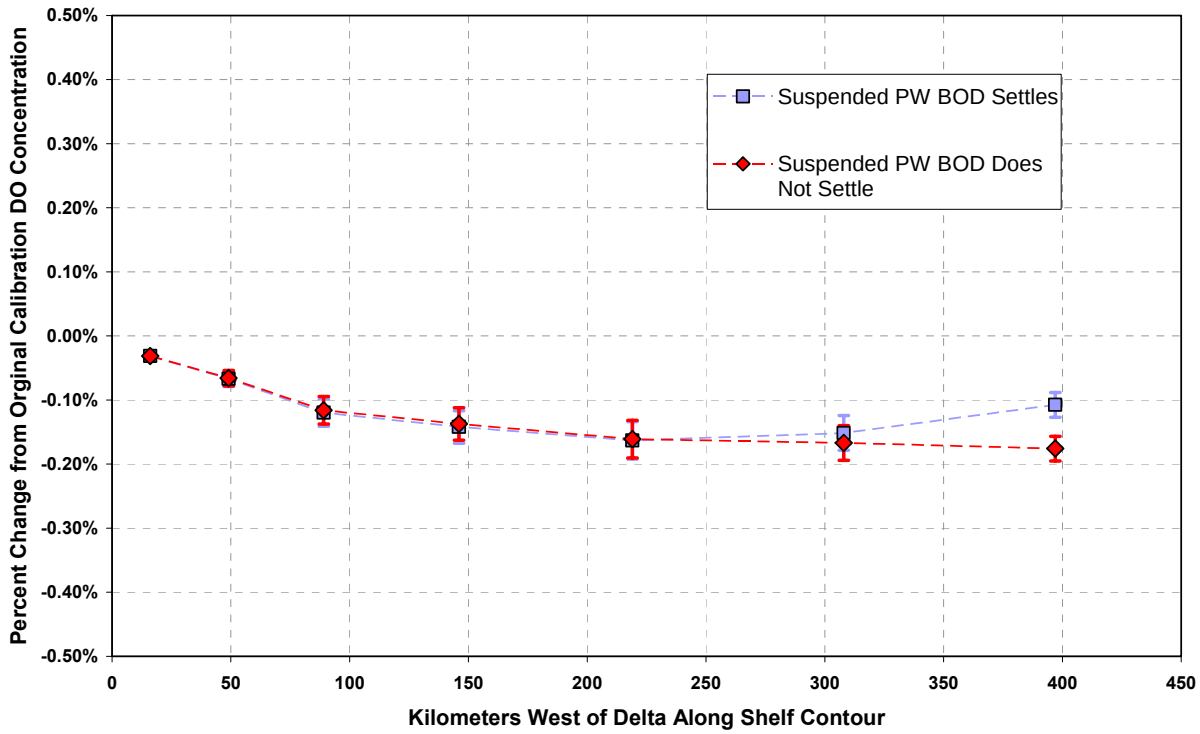

Figure 11. Predicted percent changes in bottom water dissolved oxygen concentrations for summer 1985 due to produced water loads. Results shown for base, lower bound and upper bound loads for each BOD settling case.

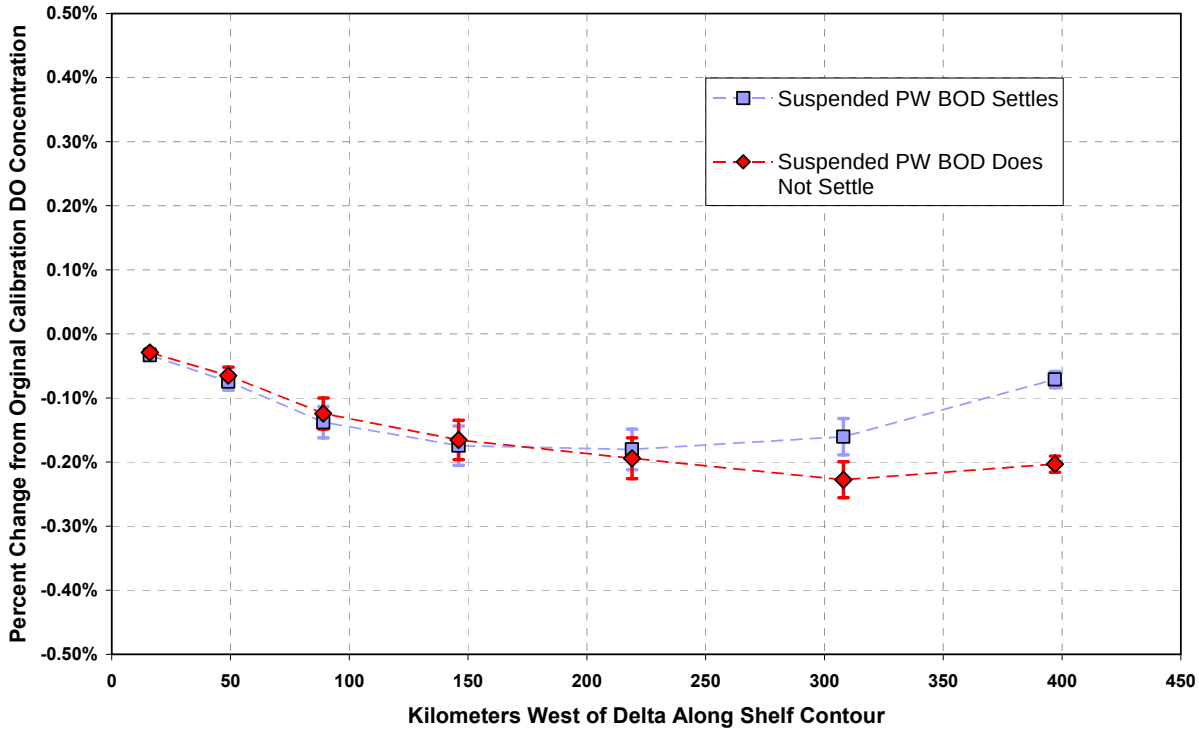

Figure 12. Predicted percent changes in bottom water dissolved oxygen concentrations for summer 1988 due to produced water loads. Results shown for base, lower bound and upper bound loads for each BOD settling case.

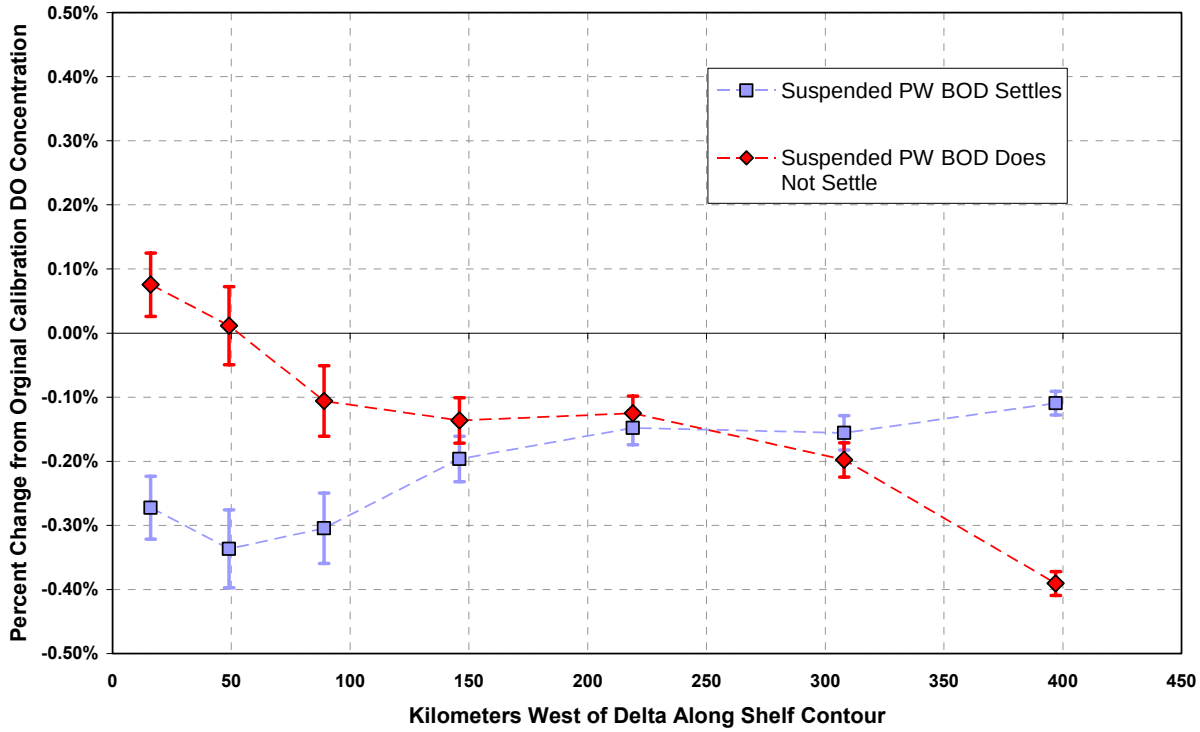

Figure 13. Predicted percent changes in bottom water dissolved oxygen concentrations for summer 1990 due to produced water loads. Results shown for base, lower bound and upper bound loads for each BOD settling case.

Figures 14-16 show predicted changes in actual bottom water DO concentrations corresponding to the predicted percent changes in Figures 11-13. For 1985 (Figure 14) and 1988 (Figure 15), the impacts of PW loads increase with distance from the delta, reach a maximum at the Atchafalaya River, and then decline further west. There is little difference between results for settling and non-settling PW BOD near the delta, but the impacts for non-settling PW BOD become greater west of the Atchafalaya. For 1990 (Figure 16) the results show different spatial patterns than for 1985 and 1988, and there are greater differences between results for settling and non-settling PW BOD. Predicted impacts for settling PW BOD are slightly greater than those for non-settling PW BOD near the delta, but cross over and become smaller west of the Atchafalaya. The predicted changes in bottom water DO concentrations due to PW loads are small. The maximum predicted changes for base PW loads were approximately 0.010 mg/L for 1985 and 1988, and 0.012 mg/L for 1990.

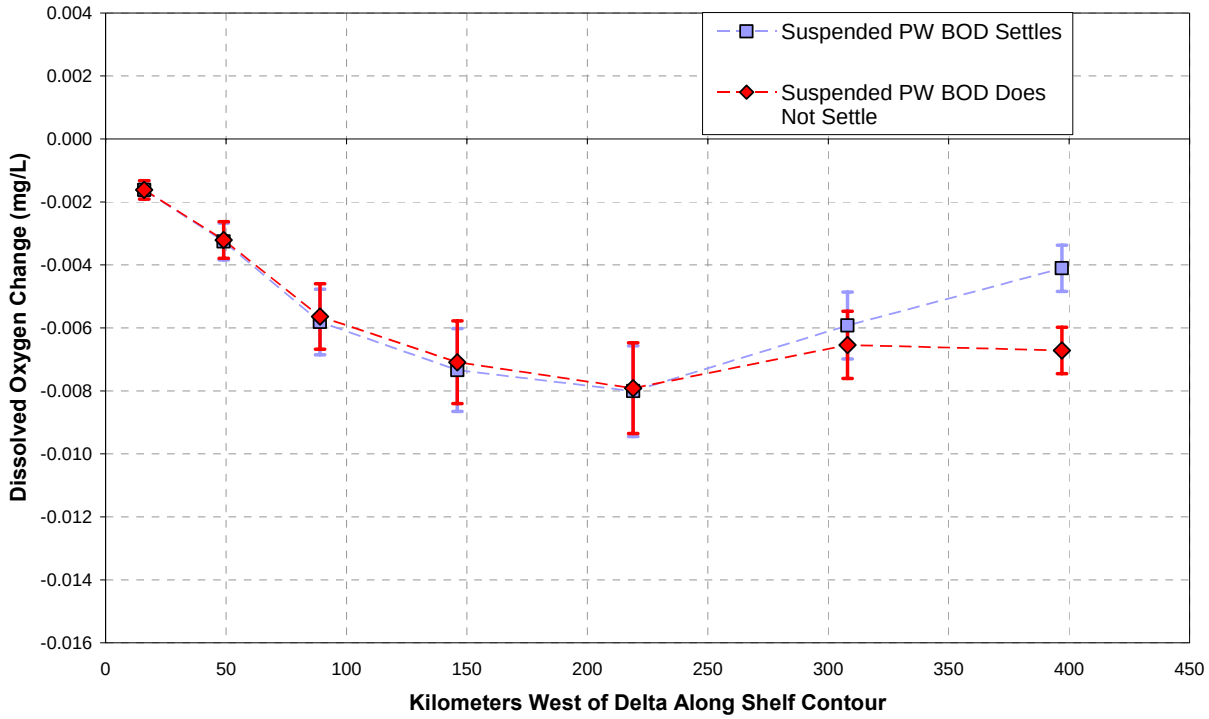

Figure 14. Predicted changes in bottom water dissolved oxygen concentrations for summer 1985 due to produced water loads. Results shown for base, lower bound and upper bound loads for each BOD settling case.

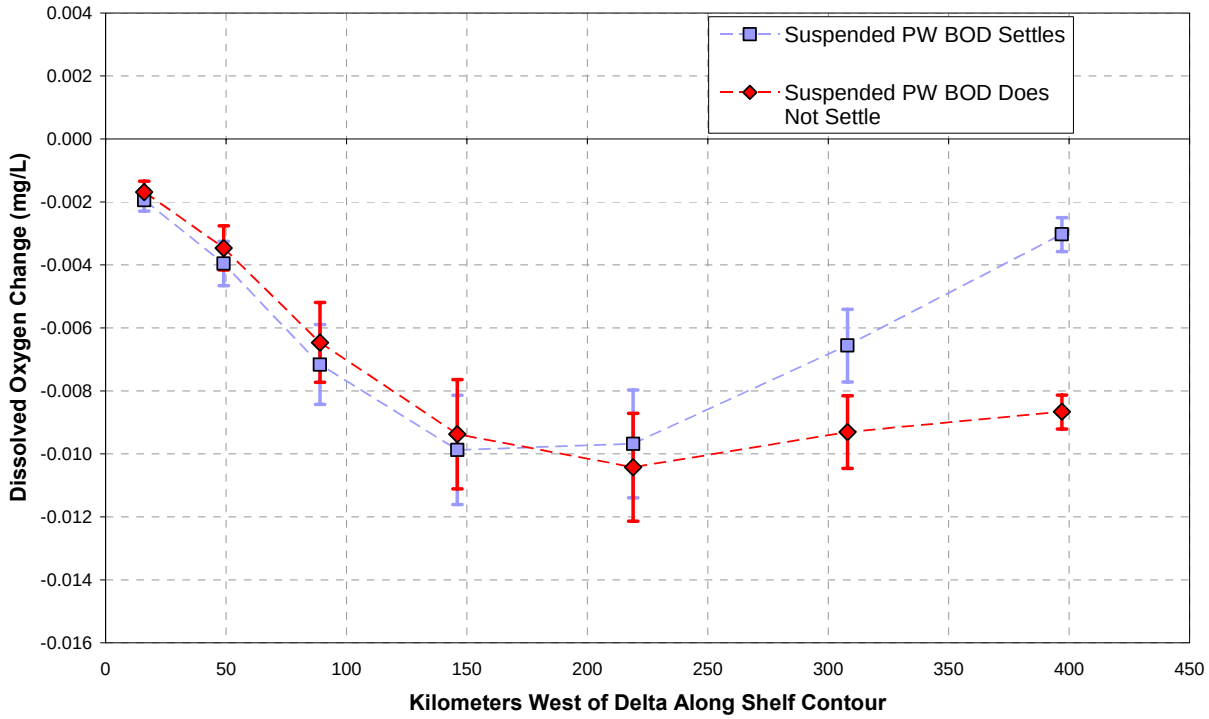

Figure 15. Predicted changes in bottom water dissolved oxygen concentrations for summer 1988 due to produced water loads. Results shown for base, lower bound and upper bound loads for each BOD settling case.

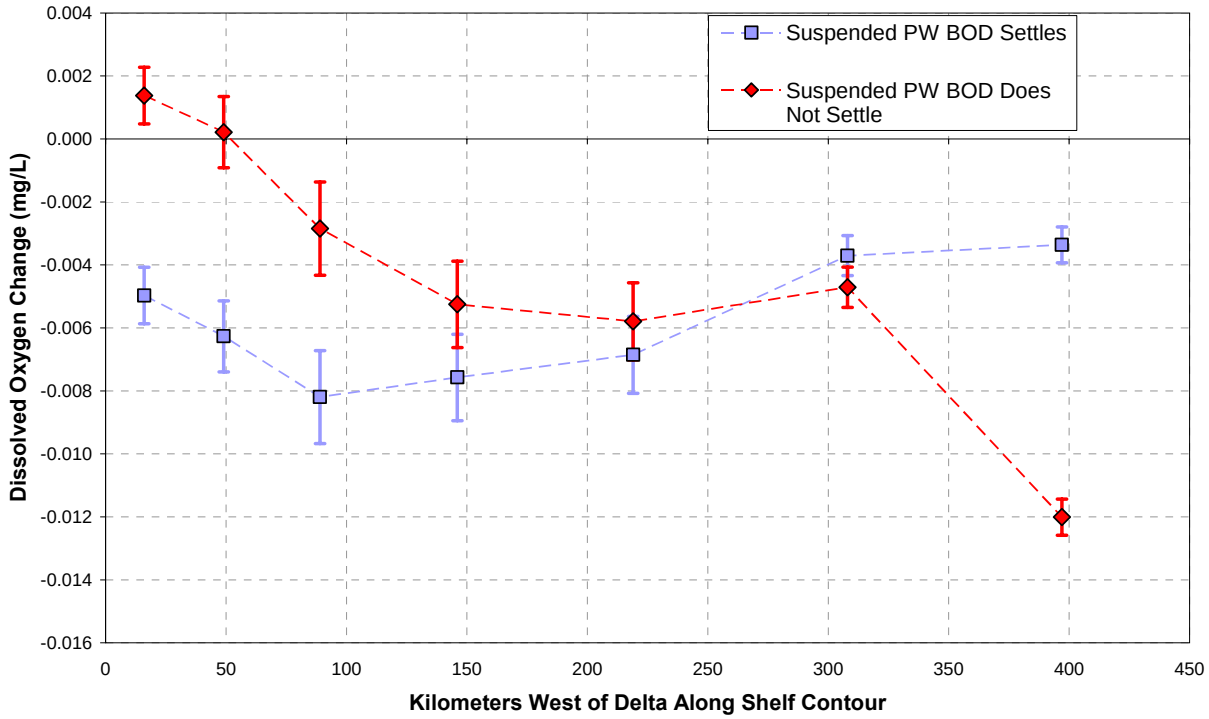

Figure 16. Predicted changes in bottom water dissolved oxygen concentrations for summer 1990 due to produced water loads. Results shown for base, lower bound and upper bound loads for each BOD settling case.

Justić Model

In the original predictions from the Justić model, bottom waters went hypoxic in 19 of 45 years from 1955 to 2000. In this study, there were no changes in frequency of hypoxia for any of the predictive simulations with PW loads. Bottom waters still went hypoxic in 19 of 45 years for all simulations. Furthermore, there were no changes in the number of months in which the bottom waters went hypoxic between the original predictions and the predictive simulations in this study.

Table 5 contains predicted average percent changes in bottom water DO concentrations from the Justić model for all scenarios. Each result corresponds to the average July-August percent change in bottom water DO concentrations at Station C6 from 1955 to 2000. As discussed below, these percent changes in bottom water DO concentrations are not constant in time, but vary over the reported period. For base PW loads delivered at the delta the average change was -0.0023 percent. For base PW loads delivered at the 10 x 10 km grid, the average change was -0.067 percent for non-settling PW TOC and -0.513 percent for settling PW TOC. The largest range across all of the lower- and upper-bound predictive simulations was from -0.0017 to -0.660 percent.

Table 5. Predicted Average Percent Changes in Summer Bottom Water Dissolved Oxygen Concentrations from the Justić Model.

	Produced Water (PW) Loads		
Scenario	**Base**	**Lower Bound**	**Upper Bound**
PW Loads (Nitrate Nitrogen) Delivered at Mississippi Delta			
Suspended PW TOC Settles	-0.0023	-0.0017	-0.0031
Suspended PW TOC Does Not Settle	N/A	N/A	N/A
PW Loads (Nitrate Nitrogen and TOC) Delivered at 10 x 10 Km Grid Centered on Station C6			
Suspended PW TOC Settles	-0.513	-0.368	-0.660
Suspended PW TOC Does Not Settle	-0.067	-0.049	-0.087

Produced Water (PW) Loads Delivered at Mississippi Delta

Figures 17a-c show predicted percent changes in monthly bottom water DO concentrations from the Justić model at Station C6 for 1955-2000. Results are included for base, lower bound and upper bound PW loads. The greatest predicted impacts occur in summer of each year. The impacts of PW loads increase with time beginning in the mid-1970s. The maximum predicted impact of base PW loads was approximately -0.016 percent for summer 1990.

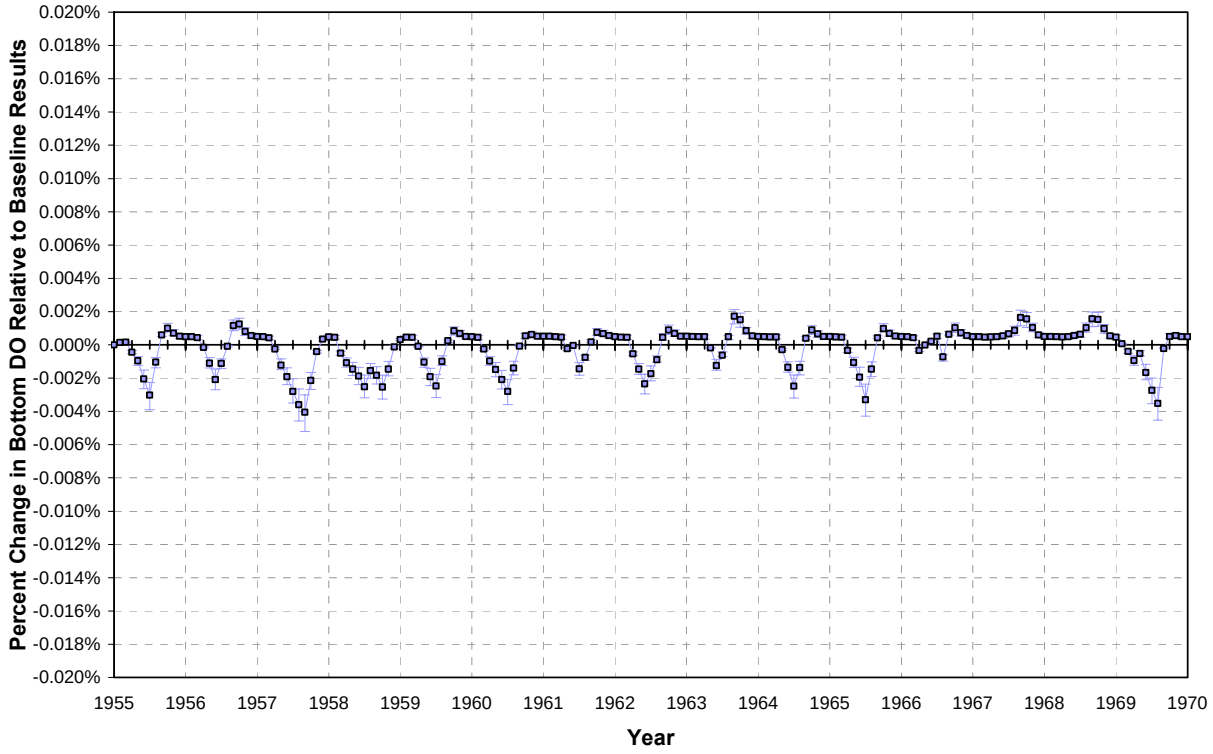

Figure 17a. Predicted percent changes in monthly bottom water dissolved oxygen concentrations at Station C6 during 1955-1970 due to produced water loads (nitrate nitrogen) delivered at the Mississippi Delta. Results shown for base, lower bound and upper bound loads.

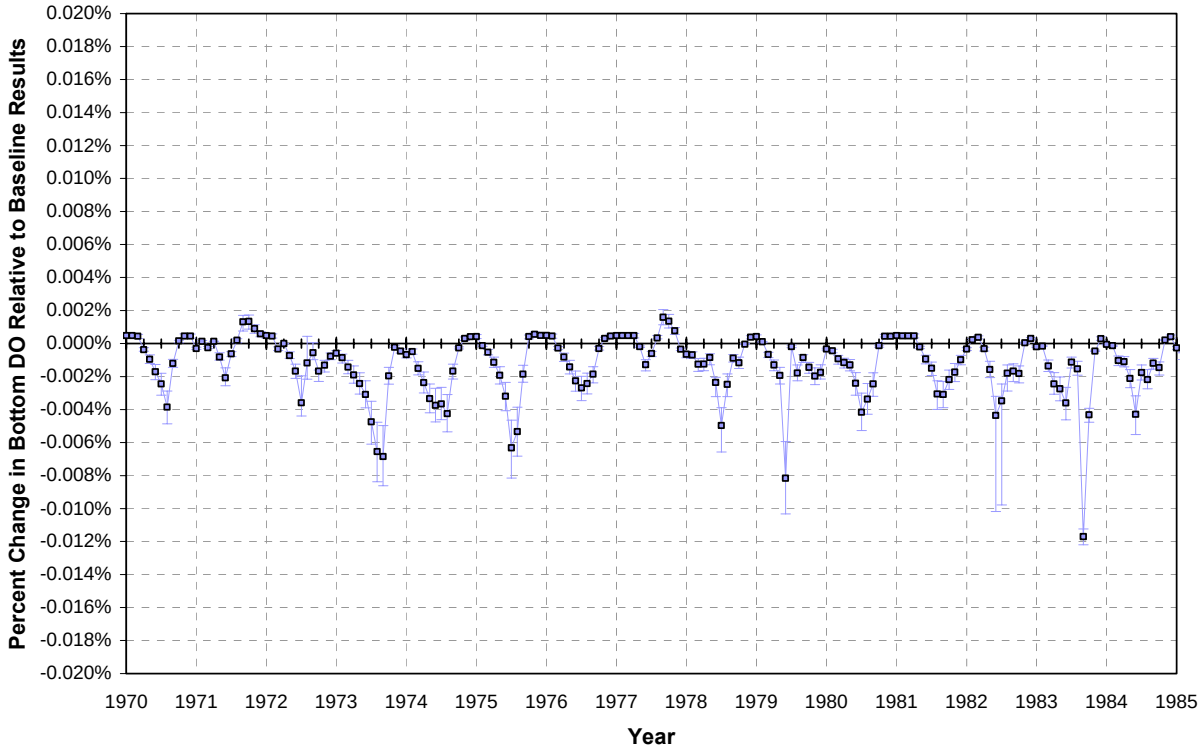

Figure 17b. Predicted percent changes in monthly bottom water dissolved oxygen concentrations at Station C6 during 1970-1985 due to produced water loads (nitrate nitrogen) delivered at the Mississippi Delta. Results shown for base, lower bound and upper bound loads.

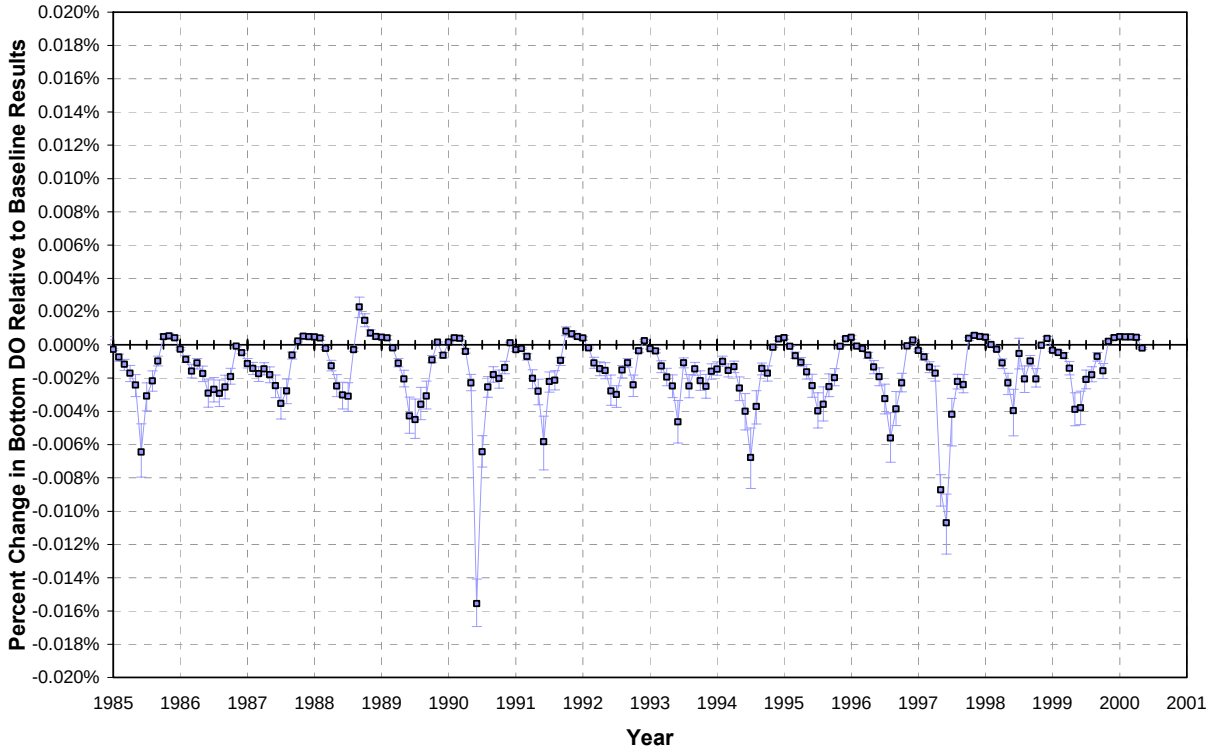

Figure 17c. Predicted percent changes in monthly bottom water dissolved oxygen concentrations at Station C6 during 1985-2001 due to produced water loads (nitrate nitrogen) delivered at the Mississippi Delta. Results shown for base, lower bound and upper bound loads.

Figures 18a-c show predicted changes in monthly bottom water DO concentrations corresponding to the predicted percent changes in Figures 17a-c. The impacts of PW loads decrease with time after the mid-1970s. The maximum predicted impact of base PW loads was approximately -0.0002 mg/L in summer 1973.

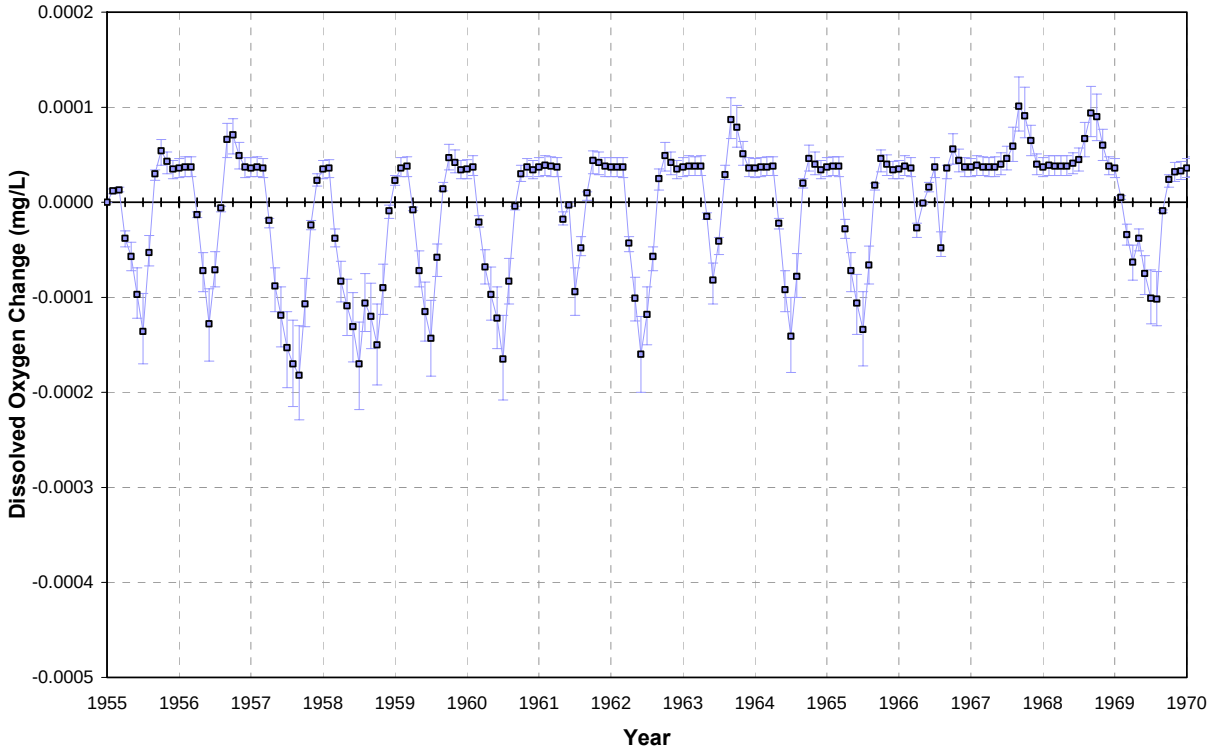

Figure 18a. Predicted changes in monthly bottom water dissolved oxygen concentrations at Station C6 during 1955-1970 due to produced water loads (nitrate nitrogen) delivered at the Mississippi Delta. Results shown for base, lower bound and upper bound loads.

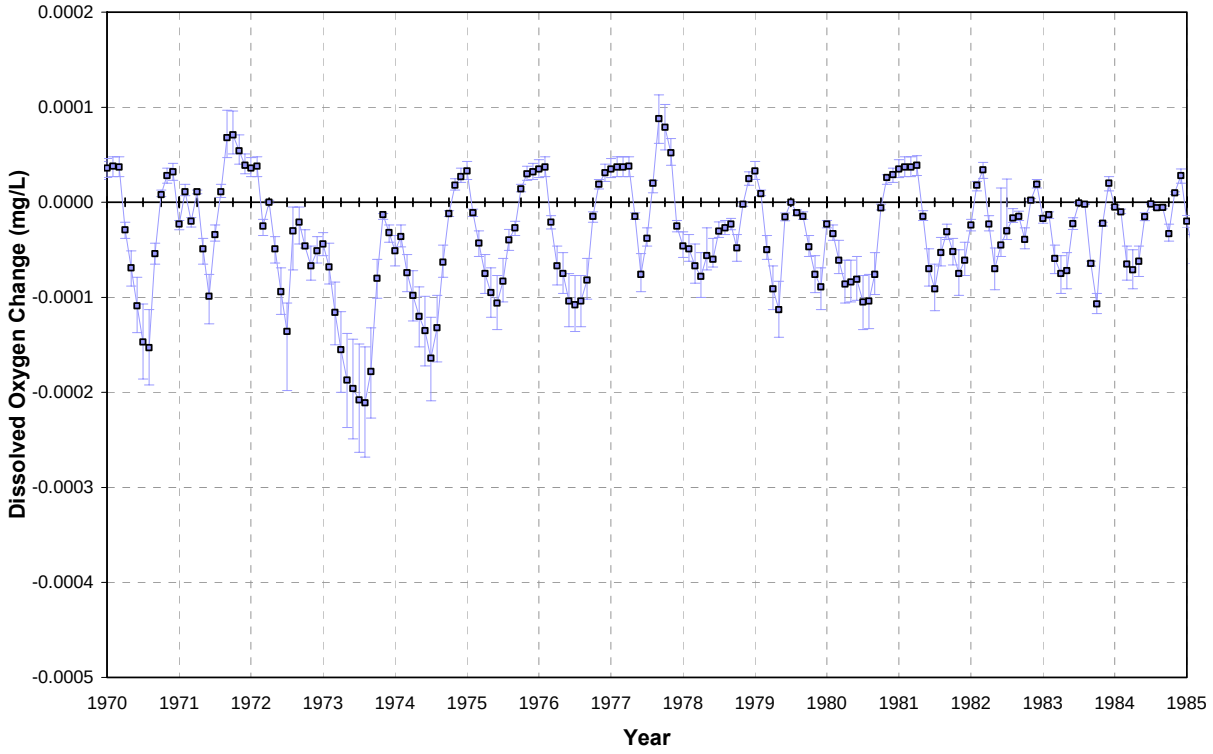

Figure 18b. Predicted changes in monthly bottom water dissolved oxygen concentrations at Station C6 during 1970-1985 due to produced water loads (nitrate nitrogen) delivered at the Mississippi Delta. Results shown for base, lower bound and upper bound loads.

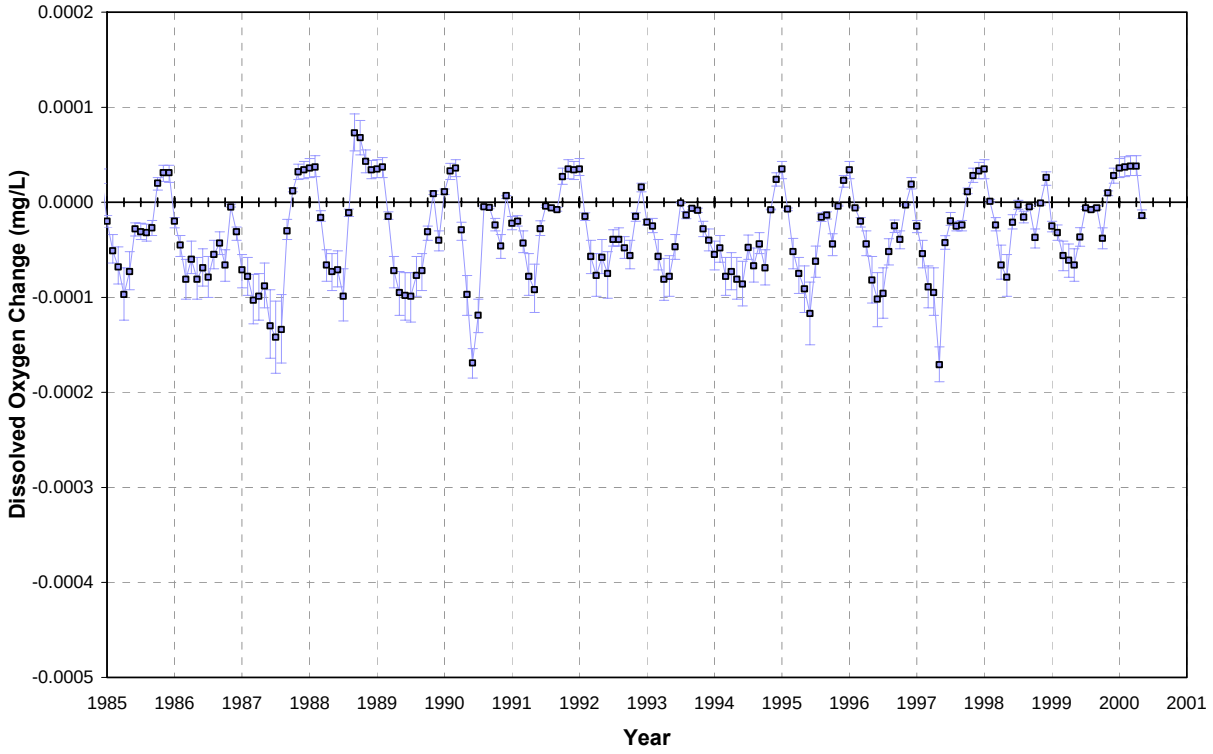

Figure 18c. Predicted changes in monthly bottom water dissolved oxygen concentrations at Station C6 during 1985-2001 due to produced water loads (nitrate nitrogen) delivered at the Mississippi Delta. Results shown for base, lower bound and upper bound loads.

Produced Water (PW) Loads Delivered at 10 x 10 Km Grid

Figures 19a-c show predicted percent changes in monthly bottom water DO concentrations from the Justić model at Station C6 for 1955-2000. Results are included for base, lower bound and upper bound PW loads. The greatest predicted impacts occur in summer of each year. The impacts of PW loads increase with time, beginning in the mid-1970s. The maximum predicted impact of base PW loads was approximately -1.4 percent for summer 1979. Impacts are substantially greater for settling PW TOC than for non-settling PW TOC, and they are outside the ranges of the PW loading uncertainties.

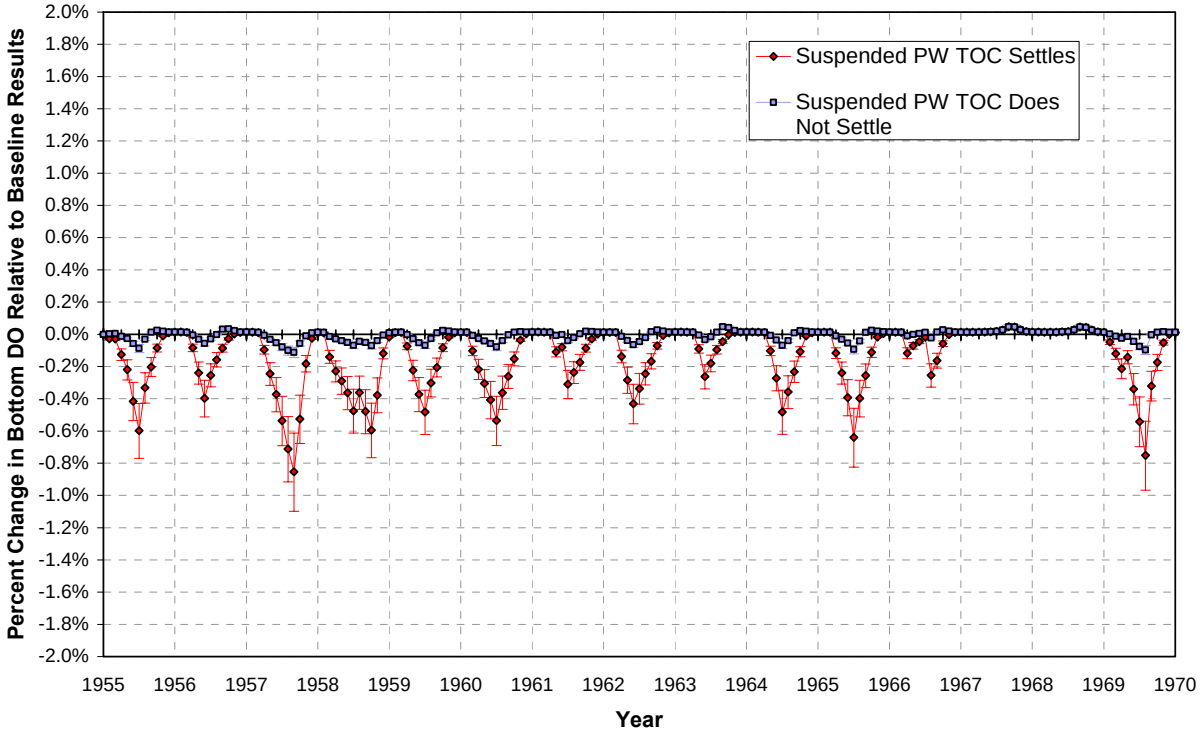

Figure 19a. Predicted percent changes in monthly bottom water dissolved oxygen concentrations at Station C6 during 1955-1970 due to produced water loads (nitrate nitrogen and TOC) delivered at the 10x10 km grid. Results shown for base, lower bound and upper bound loads for each TOC settling case.

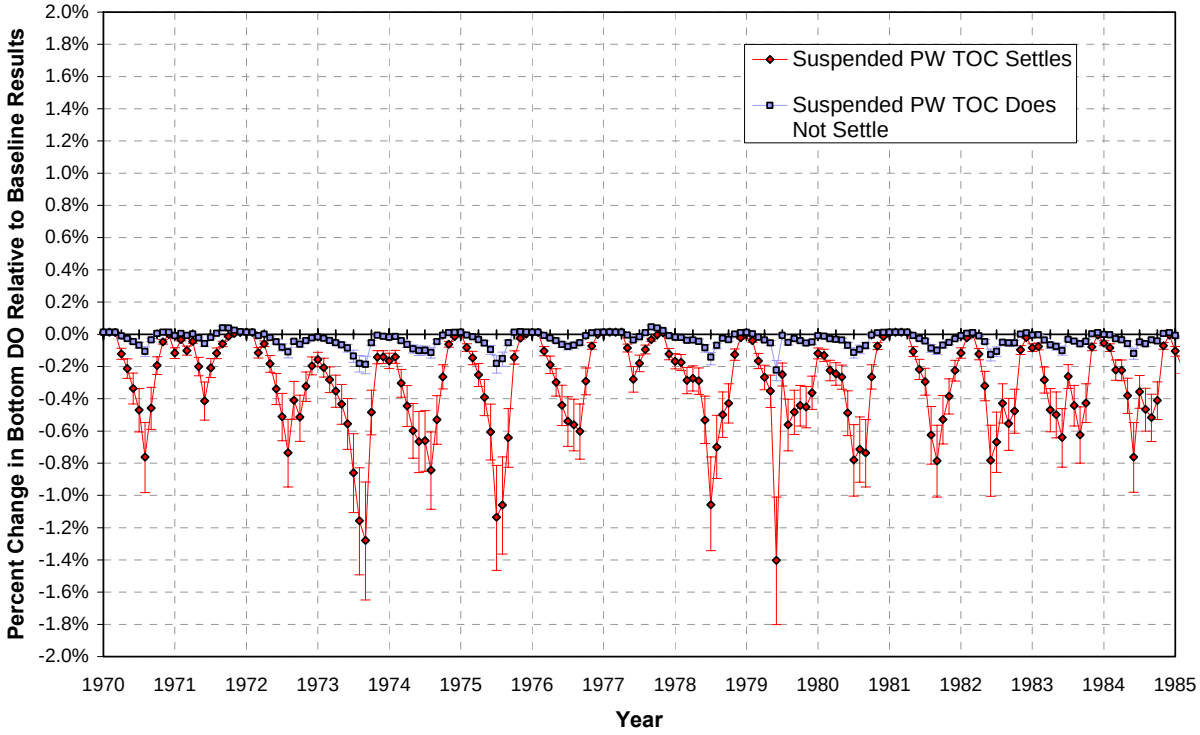

Figure 19b. Predicted percent changes in monthly bottom water dissolved oxygen concentrations at Station C6 during 1970-1985 due to produced water loads (nitrate nitrogen and TOC) delivered at the 10x10 km grid. Results shown for base, lower bound and upper bound loads for each TOC settling case.

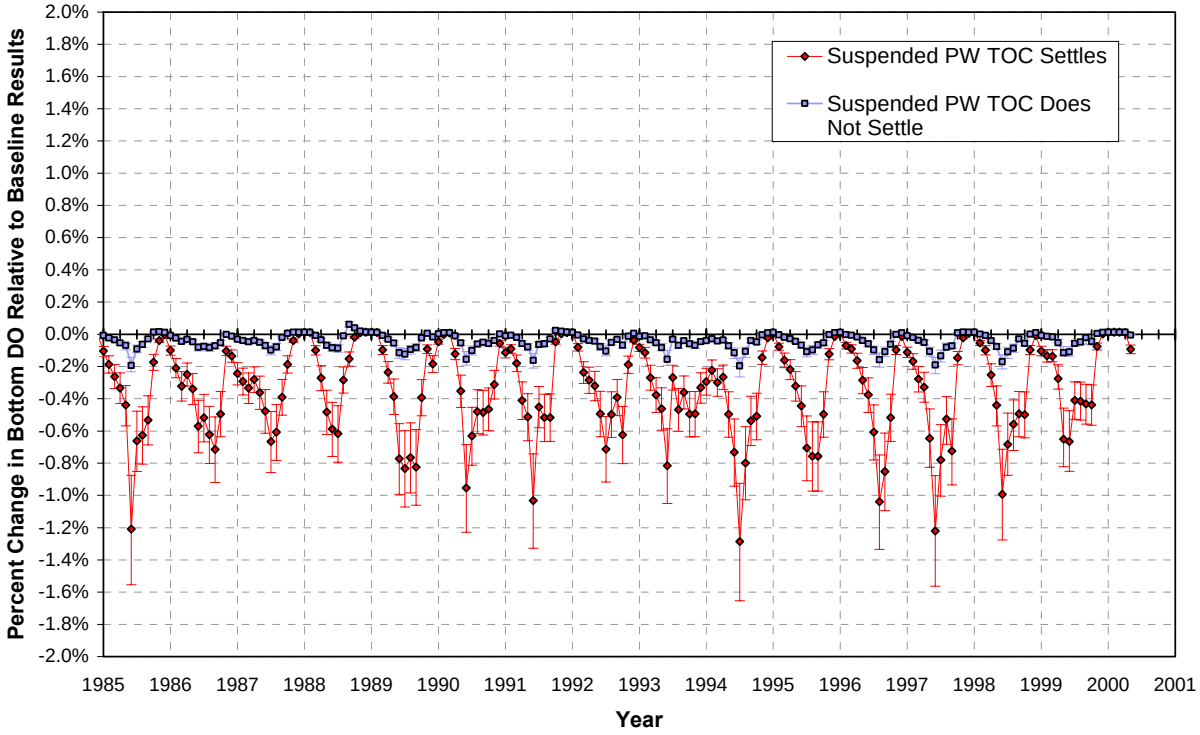

Figure 19c. Predicted percent changes in monthly bottom water dissolved oxygen concentrations at Station C6 during 1985-2001 due to produced water loads (nitrate nitrogen and TOC) delivered at the 10x10 km grid. Results shown for base, lower bound and upper bound loads for each TOC settling case.

Figures 20a-c show predicted changes in monthly bottom water DO concentrations corresponding to the predicted percent changes in Figures 19a-c. The impacts of PW loads decrease with time after the mid-1970s. The maximum predicted impact of base PW loads was approximately -0.04 mg/L in summer 1957. Impacts are substantially greater for settling PW TOC than for non-settling PW TOC, and they are outside the ranges of the PW loading uncertainties.

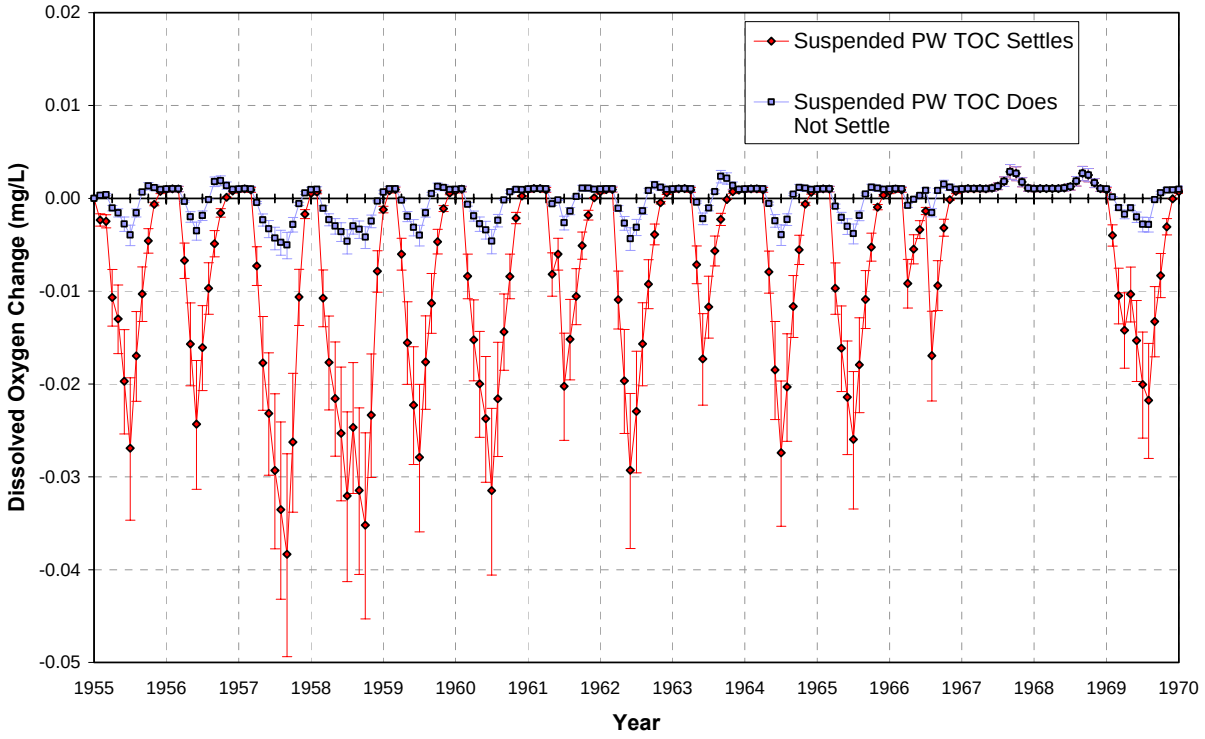

Figure 20a. Predicted changes in monthly bottom water dissolved oxygen concentrations at Station C6 during 1955-1970 due to produced water loads (nitrate nitrogen and TOC) delivered at the 10x10 km grid. Results shown for base, lower bound and upper bound loads for each TOC settling case.

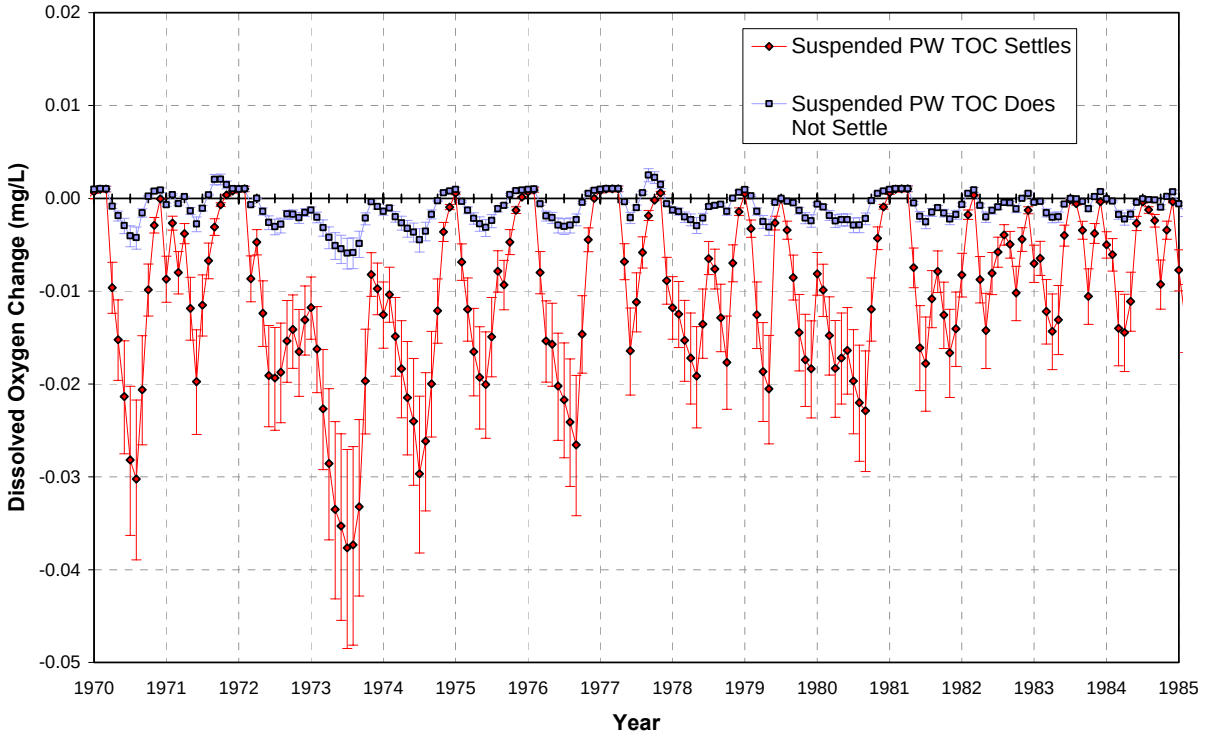

Figure 20b. Predicted changes in monthly bottom water dissolved oxygen concentrations at Station C6 during 1970-1985 due to produced water loads (nitrate nitrogen and TOC) delivered at the 10x10 km grid. Results shown for base, lower bound and upper bound loads for each TOC settling case.

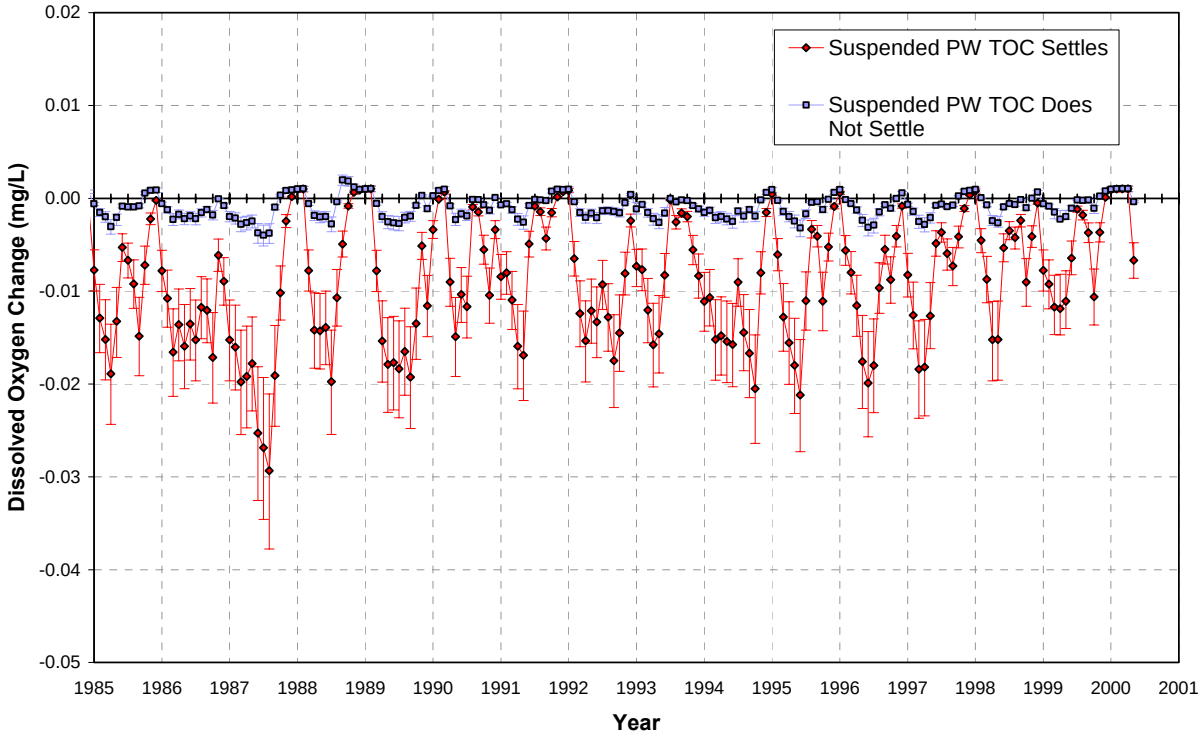

Figure 20c. Predicted changes in monthly bottom water dissolved oxygen concentrations at Station C6 during 1985-2001 due to produced water loads (nitrate nitrogen and TOC) delivered at the 10x10 km grid. Results shown for base, lower bound and upper bound loads for each TOC settling case.

Scavia Model

Produced Water (PW) Loads Delivered at Mississippi and Atchafalaya Rivers

Figure 21 shows predicted percent changes in hypoxic area from the Scavia model for 1985-2002. For base PW loads the hypoxic area increased in 3 of 18 years (1986, 1987 and 1998). The average increase was 4.5 percent and there were no differences between the settling and non-settling PW BOD cases. Predicted results for lower bound PW loads were the same as those for base PW loads. For upper bound PW loads the hypoxic area increased in 4 of 18 years (1986, 1987, 1991 and 1998). The average increase was 4.1 percent and there were no differences between the settling and non-settling PW BOD cases. As shown in Figure 22, the predicted increase in actual hypoxic area for all four of these impacted years was 331 km^2.

Produced Water Loads Delivered Along Spine of Hypoxic Zone

Figure 23 shows predicted percent changes in hypoxic area for 1985-2002. For base PW loads the hypoxic area increased in 2 of 18 years (1986 and 1991). The average increase was 3.1 percent and there were no differences between the settling and non-settling PW BOD cases. Predicted results for lower bound PW loads were the same as those for base PW loads. For upper bound PW loads the hypoxic area increased in 3 of 18 years (1986, 1991 and 1995) for settling PW BOD and in 2 of 18 years (1986, 1991) for non-settling PW BOD. The average increases were 2.8 and 3.1 percent, respectively, for these two cases. As shown in Figure 24, the predicted increase in actual hypoxic area for all three of these impacted years was 331 km^2.

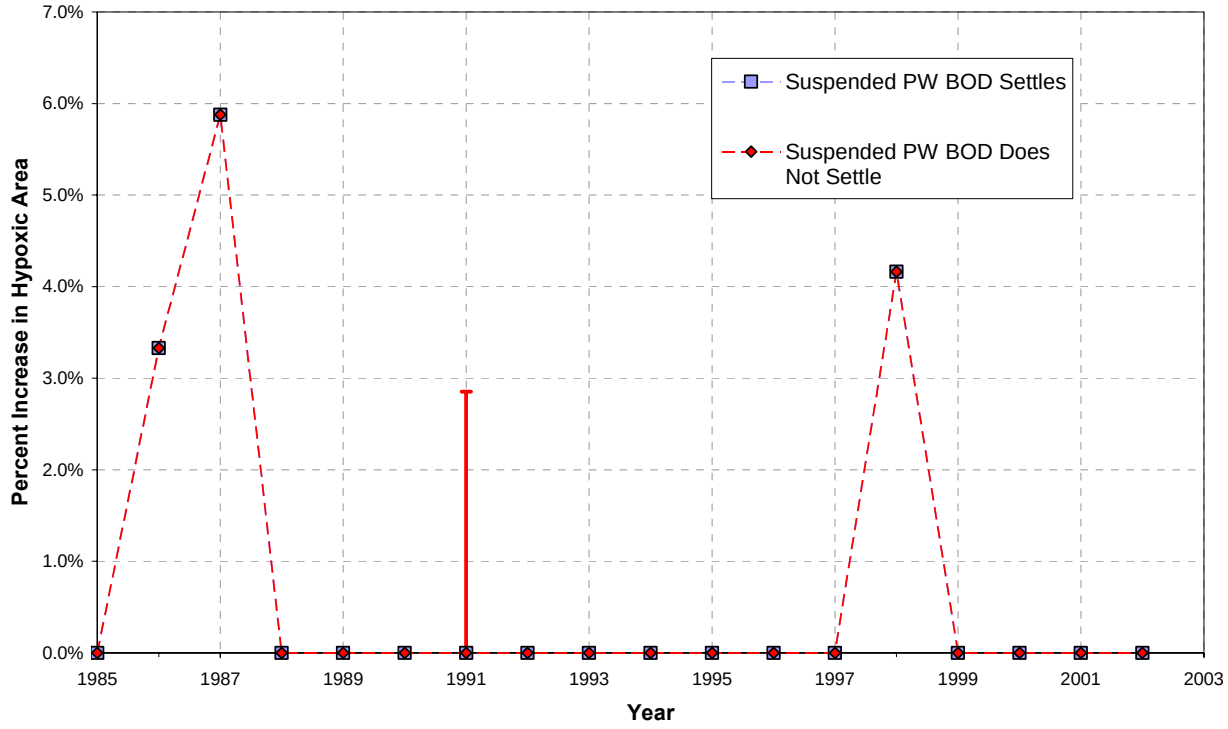

Figure 21. Predicted percent changes in hypoxic area due to produced water loads delivered at the Mississippi and Atchafalaya Rivers. Results shown for base, lower bound and upper bound loads for each BOD settling case.

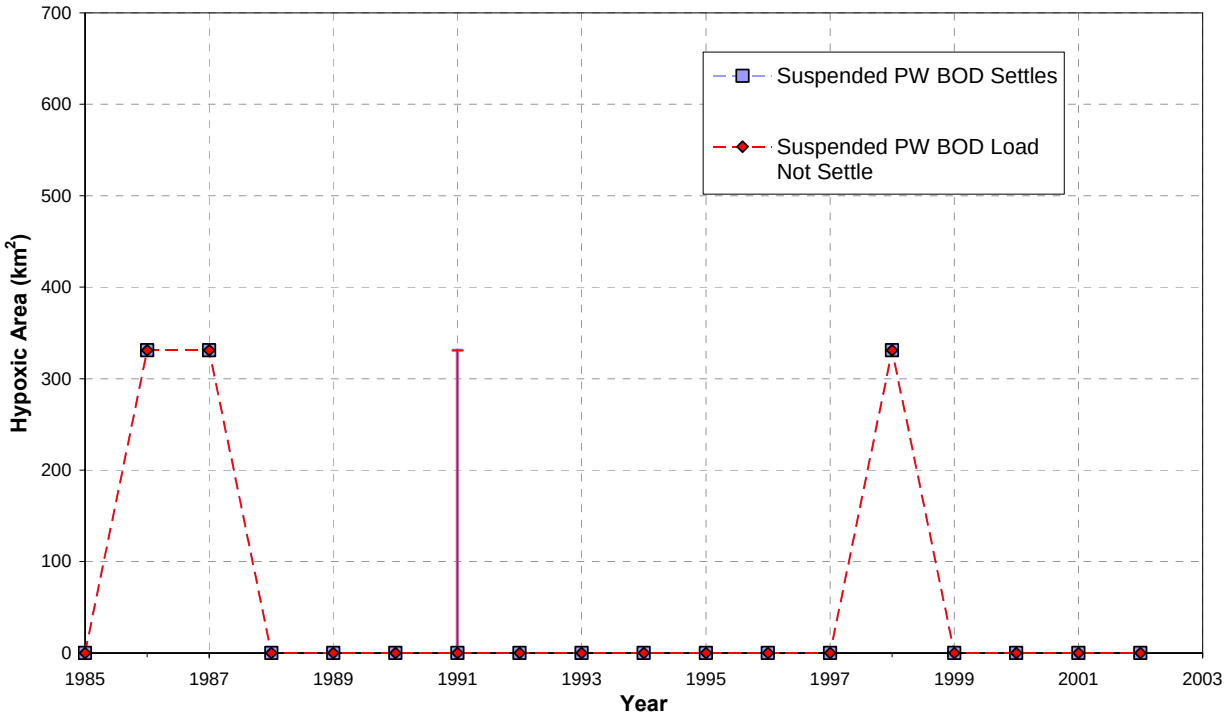

Figure 22. Predicted changes in hypoxic area due to produced water loads delivered at the Mississippi and Atchafalaya Rivers. Results shown for base, lower bound and upper bound loads for each BOD settling case.

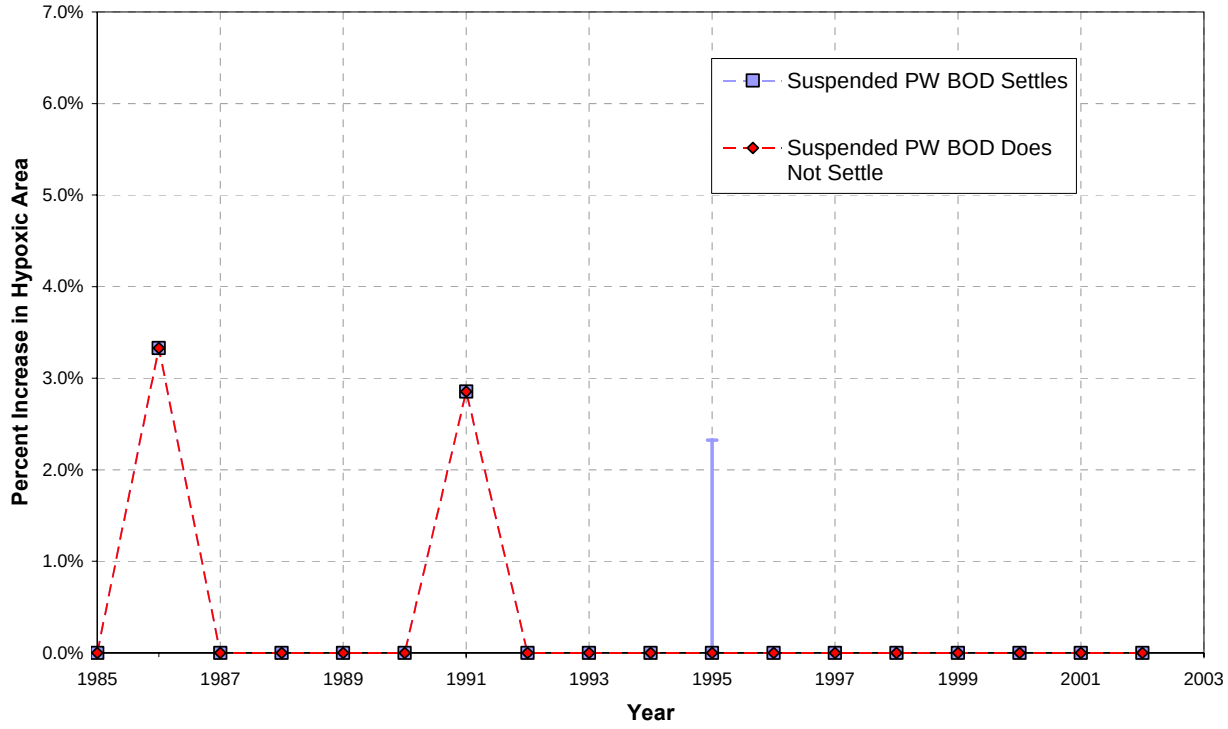

Figure 23. Predicted percent changes in hypoxic area due to produced water loads delivered at 20 km intervals along the spine of the hypoxic zone. Results shown for base, lower bound and upper bound loads for each BOD settling case.

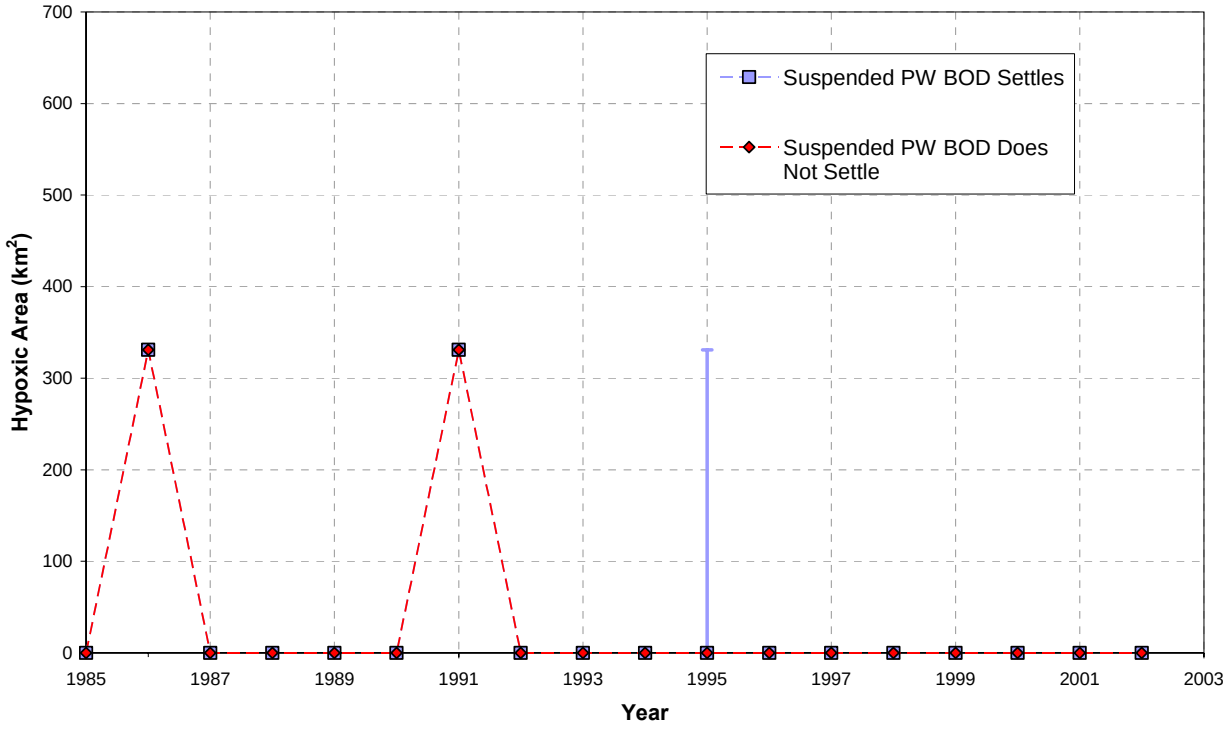

Figure 24. Predicted changes in hypoxic area due to produced water loads delivered at 20 km intervals along the spine of the hypoxic zone. Results shown for base, lower bound and upper bound loads for each BOD settling case.

DISCUSSION

The PW loads used in this study correspond only to current conditions and were assumed to be constant in time for all of the predictive simulations conducted. These simulations involved the following time periods for each of the three models: Bierman (1985, 1988, 1990), Justić (1955-2001) and Scavia (1985-2002). It should be noted that predicted impacts of PW loads for periods of time earlier than current conditions do not necessarily represent the impacts of actual PW loads during these periods.

The predictions from the Bierman model appear consistent with the relative contribution of PW loads to the northern Gulf of Mexico. Produced water loads contributed 0.16 percent of the total nitrogen loading to the northern Gulf (Table 3). For base PW loads, predicted impacts on average summer bottom water DO concentrations ranged from -0.110 to -0.201 percent for settling PW BOD and from -0.118 to -0.143 percent for non-settling PW BOD (Table 4).

The predictions from the Justić model appear consistent with the relative contribution of PW nitrate nitrogen loads to the northern Gulf of Mexico. Produced water loads contributed 0.003 percent of the total nitrate nitrogen loading to the northern Gulf (Table 3). For base PW loads

delivered at the Mississippi delta, the predicted impact on average summer bottom water DO concentrations was -0.0023 percent. It is not possible to evaluate the predictions from the Justić model for PW loads delivered at the 10 x 10 km grid in the same context because this scenario represents predicted impacts due only to near-field PW loads from lease blocks within this grid.

The predictions from the Scavia model represent area of summer hypoxia and can not be related to the relative contributions of PW loads in the same way as predictions from the Bierman and Justić models for bottom water DO concentrations. For base PW loads delivered at the Mississippi and Atchafalaya Rivers, the average predicted impact on hypoxic area was +4.5 percent; however, impacts were predicted to occur in only 3 of 18 years (1986, 1987 and 1998) and this average represents the predicted impacts in those three years. There were no predicted increases in hypoxic area for the other 15 years. For base PW loads delivered along the spine of the hypoxic zone, the averaged predicted impact on hypoxic area was +3.1 percent; however, impacts were predicted to occur in only 2 of 18 years (1986 and 1991) and this average represents the predicted impacts in those two years.

For 1990 (Figures 13 and 16) predicted results from the Bierman model show different spatial patterns than for 1985 (Figures 11 and 14) and 1988 (Figures 12 and 15), and there are greater differences between results for settling and non-settling PW BOD. These predicted differences are due to differences in the structure of the water circulation field on the Louisiana-Texas shelf (Limno-Tech, Inc. 1995). Water circulation on the shelf is strongly influenced by wind stress (Cochrane and Kelly 1986) and freshwater discharges from the MRB (Wiseman et al. 1982; Dinnel and Wiseman 1986). It is believed that summer average conditions on the shelf are typically represented by the Louisiana Coastal Current which has a net westward drift along the shelf contour. This representation is supported by current meter measurements from a long-term mooring maintained by W.J. Wiseman, Jr., formerly of Louisiana State University, at Station C6 in 20 meters of water. Typical summer average current speeds are approximately 10 and 3 cm/sec, respectively, in the surface and bottom waters.

In summer 1990 water circulation on the shelf deviated from these typical conditions and altered computed water quality responses. Net eastward drift was observed in both surface and bottom waters, and at lower speeds of approximately 2 and 0.8 cm/sec, respectively. A consequence was longer effective hydraulic detention times in each of the model spatial segments, and hence longer periods of time for degradation of organic carbon in the water column and contact between oxygen-demanding sediments and bottom waters. This interplay between altered physics and chemical-biological processes influenced the magnitude and spatial distribution of computed dissolved oxygen concentrations in bottom waters along the shelf contour.

Results from the Bierman model show that predicted impacts for non-settling PW BOD are greater than those for settling PW BOD in the region west of the Atchafalaya for all three years. This appears to be counterintuitive, but stems from the fact that there are two vertical settling fluxes for BOD in the Bierman model: (1) settling from surface to bottom waters; and (2) settling from bottom waters to the sediment bed. The settling case has greater flux of suspended phase PW BOD from surface to bottom waters than the non-settling case; however, it also has loss of suspended phase PW BOD from the bottom waters to the sediment bed. Conversely, the non-settling case has less vertical flux of suspended phase PW BOD from surface to bottom waters;

however it has no loss of suspended phase PW BOD from the bottom waters to the sediment bed. The primary driver for consumption of bottom water DO is bottom water BOD. Depending on circulation, bathymetry and location along the shelf contour, decreased vertical flux of BOD from surface to bottom waters (a BOD source) can be offset by decreased vertical flux of BOD from bottom waters to the sediment bed (a BOD sink).

For PW loads delivered at the Mississippi delta, predicted percent changes in bottom water DO concentrations from the Justić model (Figure 17a-c) increase with time beginning in the mid 1970s. This is reasonable because bottom water DO concentrations were predicted to decrease from the mid-1970s due to increases in nitrogen loads from the MRB. Conversely, predicted changes in DO concentrations (Figure 18a-c) decrease with time after the mid-1970s due to the substantial increase in nitrogen loads from the MRB beginning in the 1970s. After this period, the PW loads account for progressively smaller fractions of the total nitrogen load to the northern Gulf of Mexico.

For PW loads delivered at the 10 x 10 km grid, predicted percent changes in bottom water DO concentrations from the Justić model (Figure 19a-c) increase with time, especially since the mid-1970s. Again, this is reasonable because it coincides with the period of substantially increasing nitrogen loads from the MRB which caused decreasing DO concentrations with time. Conversely, predicted changes in DO concentrations (Figures 20a-c) decrease with time after the mid-1970s.

All of the predictive results in this study contain uncertainties inherent in each of the original models, in addition to the uncertainties explicitly considered for the produced water loads. Despite uncertainties in model results for absolute magnitudes of dissolved oxygen concentrations and hypoxic areas, relative differences between baseline and predictive simulations have higher degrees of confidence because the absolute uncertainties tend to be self-cancelling. The predicted incremental impacts of produced water loads on dissolved oxygen conditions in the northern Gulf of Mexico from all three models were small. Even considering the predicted ranges between lower- and upper-bound results, these impacts are likely to be within the errors of measurement for bottom water dissolved oxygen and hypoxic area at the spatial scale of the entire hypoxic zone.

REFERENCES

Bierman, V.J., Jr., S.C. Hinz, D. Zhu, W.J. Wiseman, Jr., N.N. Rabalais, and R.E. Turner. 1994. A preliminary mass balance model of primary productivity and dissolved oxygen in the Mississippi River plume/inner Gulf Shelf region. Estuaries 17: 886–99.

Chapra, S.C. 1997. Surface Water-Quality Modeling, McGraw-Hill, Boston.

Cochrane, J.D. and F.J. Kelly. 1986. Low-frequency circulation on the Texas-Louisiana continental shelf. Journal of Geophysical Research. 91(C9):10,645-10,659.

Committee on Environment and Natural Resources (CENR). 2000. Integrated Assessment of Hypoxia in the Northern Gulf of Mexico. National Science and Technology Council, Washington, D.C.

Dinnel, S.P. and W.J. Wiseman, Jr. 1986. Freshwater on the Louisiana and Texas shelf. Continental Shelf Research. 6(6):765-784.

Goolsby, D.A., W.A. Battaglin, G.B. Lawrence, R.S. Artz, B.T. Aulenbach, R.P. Hooper, D.R. Keeney and G.J. Stensland. 1999. Flux and Sources of Nutrients in the Mississippi-Atchafalaya River Basin: Topic 3 Report for the Integrated Assessment on Hypoxia in the Gulf of Mexico. NOAA Coastal Ocean Program Decision Analysis Series No. 17. NOAA Coastal Ocean Program, Silver Spring, MD. 130 pp.

Goolsby, D.A., W.A. Battaglin, B.T. Aulenbach, and R.P. Hooper. 2001. Nitrogen input to the Gulf of Mexico. J. Environ. Qual. 30: 329-336.

Justić, D., N. N. Rabalais, and R. E. Turner. 1996. Effects of climate change on hypoxia in coastal waters: a doubled CO_2 scenario for the northern Gulf of Mexico. Limnol. Oceanogr. 41: 992-1003.

Justić, D., N. N. Rabalais, and R. E. Turner. 2002. Modeling the impacts of decadal changes in riverine nutrient fluxes on coastal eutrophication near the Mississippi River Delta. Ecological Modelling 152: 33-46.

Justić, D., N. N. Rabalais, and R. E. Turner. 2003. Simulated responses of the Gulf of Mexico hypoxia to variations in climate and anthropogenic nutrient loading. Journal of Marine Systems 42: 115-126.

Limno-Tech, Inc. 1995. Estimated responses of water quality on the Louisiana Inner Shelf to nutrient load reductions in the Mississippi and Atchafalaya Rivers. Unnumbered report. Stennis Space Center, MS: U.S. Environmental Protection Agency, Gulf of Mexico Program.

Mitsch, W.J., J.W. Day Jr., J.W. Gilliam, P.M. Groffman, D.L. Hey, G.W. Randall, and N.Wang. 2001. Reducing nitrogen loading to the Gulf of Mexico from the Mississippi River basin: Strategies to counter a persistent ecological problem. BioScience 15: 373-388.

Rabalais, N.N, R.E. Turner, and D. Scavia. 2002. Beyond science into policy: Gulf of Mexico Hypoxia and the Mississippi River. BioScience 52: 129-142.

Scavia, D., N.N. Rabalais, R. E. Turner, D. Justić, and W. J. Wiseman, Jr. 2003. Predicting the response of Gulf of Mexico hypoxia to variations in Mississippi River nitrogen load. Limnol. Oceanogr. 48: 951-956.

Scavia, D., D. Justić and V.J. Bierman, Jr. 2004. Estuaries 27: 419-425.

Turner, R.E. and N.N. Rabalais. 1994. Evidence for coastal eutrophication near the Mississippi River delta. Nature. 368: 619-621.

U.S. Environmental Protection Agency. 2001. Action Plan for Reducing, Mitigating, and Controlling Hypoxia in the Northern Gulf of Mexico, Mississippi River/Gulf of Mexico Watershed Nutrient Task Force, EPA841-F-01-001, Washington, DC.

Veil, J.A., T.A. Kimmell and A.C. Rechner. 2005. Characteristics of Produced Water Discharged to the Gulf of Mexico Hypoxic Zone. Prepared for U.S. Department of Energy, National Energy Technology Laboratory, Contract W-31-109-Eng-38, Argonne National Laboratory.

Veil, J.A. 2006a. Questions from Vic Bierman to John Veil (2/28/06) and Veil's Answers (3/1/06). Technical Memorandum, March 8, 2006.

Veil, J.A. 2006b. Recommended Upper and Lower Range Values for Hypoxic Zone Sensitivity Analysis. Technical Memorandum, February 12, 2006.

Wiseman, W.J., Jr., S.P. Murray, J.M. Bane and M.W. Tubman. 1982. Temperature and salinity variability within the Louisiana Bight. Contributions in Marine Science. 25:109-120.

Appendix A

Model Linkages with Produced Water Loadings

		Year 2003 Bottom Layer (>10 m deep) Produced Water Discharge Volume (bbl)	Year 2003 Surface Layer (<10 m deep) Produced Water Discharge Volume (bbl)	Average Produced Water Concentrations (mg/L) (Veil et al. 2005)															
				585.4		229.1		1.11		0.05		77.63		83.59		0.368		0.612	
				Bottom BOD_5 Load (lb/day)	Surface BOD_5 Load (lb/day)	Bottom TOC Load (lb/day)	Surface TOC Load (lb/day)	Bottom Nitrate-N Load (lb/day)	Surface Nitrate-N Load (lb/day)	Bottom Nitrite-N Load (lb/day)	Surface Nitrite-N Load (lb/day)	Bottom Ammonia-N Load (lb/day)	Surface Ammonia-N Load (lb/day)	Bottom TKN Load (lb/day)	Surface TKN Load (lb/day)	Bottom Ortho-P Load (lb/day)	Surface Ortho-P Load (lb/day)	Bottom TP Load (lb/day)	Surface TP Load (lb/day)
Spatial Representation	**Spatial ID**																		
EPA Hypoxic Zone	**Veil et al. (2005)**	**59,981,762**	**125,340,459**	33,691	70,403	13,185	27,553	63.9	133.5	2.88	6.01	4,468	9,336	4,811	10,053	21.2	44.3	35.2	73.6
	Grand Total		**185,322,221**		**104,095**		**40,738**		**197.4**		**8.89**		**13,804**		**14,864**		**65.4**		**108.8**
Bierman Model Surface Segment	**1**	0	3,877,932	0	2,178	0	852	0.0	4.1	0.00	0.19	0	289	0	311	0.0	1.4	0.0	2.3
	2	821,918	65,995	462	37	181	15	0.9	0.1	0.04	0.00	61	5	66	5	0.3	0.0	0.5	0.0
	3	0	8,464,293	0	4,754	0	1,861	0.0	9.0	0.00	0.41	0	630	0	679	0.0	3.0	0.0	5.0
	4	0	8,726,377	0	4,902	0	1,918	0.0	9.3	0.00	0.42	0	650	0	700	0.0	3.1	0.0	5.1
	5	1,070,738	6,357,152	601	3,571	235	1,397	1.1	6.8	0.05	0.30	80	474	86	510	0.4	2.2	0.6	3.7
	6	67,178	1,663,925	38	935	15	366	0.1	1.8	0.00	0.08	5	124	5	133	0.0	0.6	0.0	1.0
	7	0	2,478,976	0	1,392	0	545	0.0	2.6	0.00	0.12	0	185	0	199	0.0	0.9	0.0	1.5
	8	12,649,144	3,137,344	7,105	1,762	2,781	690	13.5	3.3	0.61	0.15	942	234	1,015	252	4.5	1.1	7.4	1.8
	9	13,671,291	10,724,066	7,679	6,024	3,005	2,357	14.6	11.4	0.66	0.51	1,018	799	1,097	860	4.8	3.8	8.0	6.3
	10	11,652,550	30,156,237	6,545	16,939	2,562	6,629	12.4	32.1	0.56	1.45	868	2,246	935	2,419	4.1	10.6	6.8	17.7
	11	0	19,649,404	0	11,037	0	4,319	0.0	20.9	0.00	0.94	0	1,464	0	1,576	0.0	6.9	0.0	11.5
	12	2,267,574	28,264,337	1,274	15,876	498	6,213	2.4	30.1	0.11	1.36	169	2,105	182	2,267	0.8	10.0	1.3	16.6
	13	2,004,887	8,393,186	1,126	4,714	441	1,845	2.1	8.9	0.10	0.40	149	625	161	673	0.7	3.0	1.2	4.9
	14	556,167	8,601,550	312	4,831	122	1,891	0.6	9.2	0.03	0.41	41	641	45	690	0.2	3.0	0.3	5.1
	Subtotal	**44,761,447**	**140,560,774**	**25,142**	**78,952**	**9,840**	**30,899**	**47.7**	**149.7**	**2.15**	**6.74**	**3,334**	**10,470**	**3,590**	**11,274**	**15.8**	**49.6**	**26.3**	**82.5**
	Grand Total		**185,322,221**		**104,095**		**40,738**		**197.4**		**8.89**		**13,804**		**14,864**		**65.4**		**108.8**
Scavia Model Loading Point KM	**10**	953,279	537,617	535	302	210	118	1.0	0.6	0.05	0.03	71	40	76	43	0.3	0.2	0.6	0.3
	30	15,494,072	8,738,137	8,703	4,908	3,406	1,921	16.5	9.3	0.74	0.42	1,154	651	1,243	701	5.5	3.1	9.1	5.1
	50	8,917,767	4,351,023	5,009	2,444	1,960	956	9.5	4.6	0.43	0.21	664	324	715	349	3.1	1.5	5.2	2.6
	70	19,121,015	173,689	10,740	98	4,203	38	20.4	0.2	0.92	0.01	1,424	13	1,534	14	6.8	0.1	11.2	0.1
	90	2,794,901	15,307,755	1,570	8,598	614	3,365	3.0	16.3	0.13	0.73	208	1,140	224	1,228	1.0	5.4	1.6	9.0
	110	0	17,948,995	0	10,082	0	3,946	0.0	19.1	0.00	0.86	0	1,337	0	1,440	0.0	6.3	0.0	10.5
	130	0	7,079,153	0	3,976	0	1,556	0.0	7.5	0.00	0.34	0	527	0	568	0.0	2.5	0.0	4.2
	150	0	12,777,740	0	7,177	0	2,809	0.0	13.6	0.00	0.61	0	952	0	1,025	0.0	4.5	0.0	7.5
	170	0	9,401,408	0	5,281	0	2,067	0.0	10.0	0.00	0.45	0	700	0	754	0.0	3.3	0.0	5.5
	190	0	7,979,866	0	4,482	0	1,754	0.0	8.5	0.00	0.38	0	594	0	640	0.0	2.8	0.0	4.7
	210	2,500,693	7,773,560	1,405	4,366	550	1,709	2.7	8.3	0.12	0.37	186	579	201	623	0.9	2.7	1.5	4.6
	230	408,149	9,992,599	229	5,613	90	2,197	0.4	10.6	0.02	0.48	30	744	33	801	0.1	3.5	0.2	5.9
	250	990,716	7,857,728	556	4,414	218	1,727	1.1	8.4	0.05	0.38	74	585	79	630	0.3	2.8	0.6	4.6
	270	0	2,081,887	0	1,169	0	458	0.0	2.2	0.00	0.10	0	155	0	167	0.0	0.7	0.0	1.2
	290	265,365	539,394	149	303	58	119	0.3	0.6	0.01	0.03	20	40	21	43	0.1	0.2	0.2	0.3
	310	1,467,454	2,406,365	824	1,352	323	529	1.6	2.6	0.07	0.12	109	179	118	193	0.5	0.8	0.9	1.4
	330	254,830	1,541,954	143	866	56	339	0.3	1.6	0.01	0.07	19	115	20	124	0.1	0.5	0.1	0.9
	350	52,465	3,975,952	29	2,233	12	874	0.1	4.2	0.00	0.19	4	296	4	319	0.0	1.4	0.0	2.3
	370	0	4,366,514	0	2,453	0	960	0.0	4.7	0.00	0.21	0	325	0	350	0.0	1.5	0.0	2.6
	390	0	3,801,726	0	2,135	0	836	0.0	4.0	0.00	0.18	0	283	0	305	0.0	1.3	0.0	2.2
	410	556,093	1,991,148	312	1,118	122	438	0.6	2.1	0.03	0.10	41	148	45	160	0.2	0.7	0.3	1.2
	430	0	876,113	0	492	0	193	0.0	0.9	0.00	0.04	0	65	0	70	0.0	0.3	0.0	0.5
	450	0	45,099	0	25	0	10	0.0	0.0	0.00	0.00	0	3	0	4	0.0	0.0	0.0	0.0
	Subtotal	**53,776,800**	**131,545,421**	**30,206**	**73,889**	**11,821**	**28,917**	**57.3**	**140.1**	**2.58**	**6.31**	**4,006**	**9,798**	**4,313**	**10,551**	**19.0**	**46.4**	**31.6**	**77.2**
	Grand Total		**185,322,221**		**104,095**		**40,738**		**197.4**		**8.89**		**13,804**		**14,864**		**65.4**		**108.8**
Justic Model C6 Spatial Zone	**10 km Grid**	0	14,377,162	0	8,076	0	3,160	0.0	15.3	0.00	0.69	0	1,071	0	1,153	0.0	5.1	0.0	8.4
	Grand Total		**14,377,162**		**8,076**		**3,160**		**15.3**		**0.69**		**1,071**		**1,153**		**5.1**		**8.4**
	C6 to MAR	46,975,786	40,332,465	26,386	22,655	10,326	8,866	50.0	43.0	2.25	1.93	3,499	3,004	3,768	3,235	16.6	14.2	27.6	23.7
	Grand Total		**87,308,251**		**49,041**		**19,192**		**93.0**		**4.19**		**6,503**		**7,003**		**30.8**		**51.3**